Simulation of a Quantum Annealer

von

Ting-Jui Hsu

Masterarbeit in Simulation Sciences

vorgelegt der

Fakultät für Maschinenwesen

der RWTH Aachen

im July 2017

angefertigt am

Jülich Supercomputing Center
Forschungszentrum Jülich

bei

Prof. Dr. Kristel Michielsen

Abstract

In this study, we simulated a quantum annealing process at zero and finite temperature by using the full diagonalisation method and the Suzuki-Trotter product formula approach. We used quantum annealing to solve the 2-satisfiability problem. We have demonstrated that the probability for finding the solution depends not only on the total annealing time, the minimum gap between the ground state energy and the first excited state energy of the system during the annealing process, but also on the temperature.

Contents

1 Introduction **2**

2 Theory of Quantum Annealing **4**
2.1 Quantum Annealing and Adiabatic Quantum Computation 4
2.2 Adiabatic Theorem 8
2.3 Landau-Zener Transition 9

3 Optimisation Problems **11**
3.1 Combinatorial Optimisation 11
3.2 Boolean Satisfiability Problems 12
3.3 Mapping the 2-SAT Problem to the Ising Hamiltonian 13

4 Simulation Algorithms **14**
4.1 The Time-Dependent Schrödinger Equation and the Quantum Spin System 14
4.2 Algorithms for a System at Zero Temperature 16
4.2.1 The Full Diagonalisation Method 16
4.2.2 The Suzuki-Trotter Product Formula Approach 16
4.3 Algorithms for a System at Finite Temperature 20
4.3.1 Canonical Ensemble 20
4.3.2 The Random Sampling Method 20

5 Simulation Results for a Quantum Annealer at Zero Temperature **23**
5.1 The Evolution of the Energy, the Success Probability, and the Spin Value . 23
5.2 The Effect of the Total Annealing Time 23
5.3 The Effect of the Minimum Gap 26

6 Simulation Results for a Quantum Annealer at Finite Temperature **30**
6.1 Validation of the Random Sampling Method 30
6.2 The Effect of the Temperature 30
6.3 The Effect of the Minimum Gap 32

7 Applications on Machine Learning **37**

8 Conclusion **40**

1 Introduction

The idea of quantum computation was brought up in the early 80s [1]. Feynman thought that a simulation of quantum phenomena is not always feasible on a classical computer, because the amount of resources required for the computation grows exponentially with the size of the physical system. Instead, quantum phenomena should be simulated by a computer making use of quantum properties, with which the amount of resources required for the simulation is only proportional to the size of the physical system.

After this idea, an interesting topic for scientists is how computation can benefit from storing, transferring and processing information with quantum properties. Quantum computation is expected to do more than just simulation of quantum phenomena. Some quantum algorithms were presented and shown to have a significant speed-up compared to classical ones. Here follow some examples. Simon's algorithm can reduce the run time from an exponential time on a classical computer to a polynomial time on a quantum computer when solving a black box problem [2]. Furthermore, this also serves as the stepping-stone to Shor's Algorithm. Shor's Algorithm for factorising large integers is one of the most well-known quantum algorithms. The time it takes to factorise an n-bit number grows as a polynomial in n on a quantum computer. The time for the same task grows exponentially with n on a classical computer [3]. The toughness of the factorising problem is the basis of many cryptography techniques and information is usually encrypted and protected by a large semi prime number. Therefore, some classical cryptography algorithms, like RSA, seems to break down and quantum cryptography is under research as a response to this. The last one is Grover's search algorithm. To search an item in an unstructured list of size N costs a classical computer run time of the order of N. Grover's algorithm can solve the same task in the order of $\sqrt{N}$ [4]. Not like Shor's algorithm, which has an exponential speed-up, Grover's algorithm has only a quadratic improvement. It is still an important algorithm because of its broad applications, such as to speedup the time required to solve NP-complete problems [5, 6].

All algorithms mentioned above are expected to run on a universal quantum computer, which is usually referred to as a machine based on the quantum gate model. However, building a quantum gate computer may be a challenging task. The main difficulty comes from the close box requirement [7]. The quantum system of a quantum computer should be isolated from its environment while being controlled. The quantum system is so fragile that even a little amount of noise can cause harm to the system, known as decoherence. Furthermore, due to the environmental noise, the entropy of the system will keep increasing with time. Therefore, there must exist a way to cool the quantum system and maintain its quantum state. How to measure results is another important issue, because the computational result makes sense only when it can be measured. Also, the possibility to scale up the system is crucial. A universal quantum computation can be implemented only when the above requirements on the hardware are fulfilled.

Another approach to universal quantum computation is adiabatic quantum computation. While the computation based on the quantum gate model is encoded into a series of

quantum logic gates, adiabatic quantum computation proceeds from an initial Hamiltonian to a final Hamiltonian, which encodes the solution of the desired problem. There are debates on whether adiabatic quantum computation can be considered as universal quantum computation. It has been shown that the model of adiabatic quantum computation differs from the standard model of universal quantum computation within a polynomial time [8, 9]. It implies that adiabatic quantum computation and the computation based on the quantum gate model can simulate each other with a polynomial overhead. Some criticised that this only holds under ideal circumstances without noise. There are effective models for building a fault-tolerant gate based quantum computer. By contrast, whether fault-tolerance is possible on a quantum annealer is unknown [10].

With the idea of encoding the solution of combinatorial optimisation to a Hamiltonian, quantum annealing is considered as a special kind of adiabatic quantum computation. An experimental implementation of quantum annealing in a disordered magnet in 1999 [11] demonstrated a possibility to design hardware, namely a quantum annealer, that solves optimisation problems by quantum evolution. In the same year, D-wave Systems Inc. was established. D-Wave Systems Inc. is a company which focuses on building a quantum annealer and the target is optimisation. D-wave Systems Inc. released the first commercial system in 2010 with 128 qubits. The latest system is D-Wave 2000Q with 2048 qubits. By emphasising on optimisation, a quantum annealer has potential application in fields like machine learning, pattern recognition, and computer vision. Based on this, the quantum annealer is sometimes considered to be specialised in optimisation only instead of being a universal quantum computer.

The 2-satisfiability problem is investigated in this report. A 2-satisfiability problem can be expressed as a Boolean formula. This Boolean formula is constructed by a series of conjunctions of clauses. Each clause contains 2 Boolean variables at most. The aim of the problem is to find a configuration that makes the Boolean formula true. Once a 2-satisfiability problem is mapped to a problem Hamiltonian, it can be solved on a quantum annealer. The probability of finding the correct ground state after annealing is expected to increase when increasing the total annealing time. This is the case in ideal conditions, which corresponds to a quantum system at zero temperature. However, when a quantum annealing process is done at finite temperature, this probability does not increase monotonically.

The outline of the report is as follows. In section 2, the general idea of quantum annealing and the theory behind it is introduced. Section 3 presents the definition and the characteristics of optimisation problems. Section 4 provides the algorithms used for the simulation of a spin-system. In Section 5 and section 6, the simulation results of an ideal system and a system with temperature effect will be discussed respectively. Section 7 is about the applications of quantum annealing in the field of machine learning. Section 8 contains the conclusion.

2 Theory of Quantum Annealing

2.1 Quantum Annealing and Adiabatic Quantum Computation

Before going into quantum annealing, it is worth mentioning the reason why using the annealing technique in general and what is the difference between simulated annealing and quantum annealing. The annealing technique is used because of the properties of combinatorial optimisation. The goal of combinatorial optimisation is to find an optimal solution among a finite set of candidate solutions. The set of candidate solutions is discrete. A brute-force search for the optimal one is not practical on a classical computer when the problem size is large. To reduce the run time of it, one possible method is annealing. If one can encode the problem into a cost function of which the minimum value corresponds to the solution of the optimisation problem, an annealing algorithm can help to find the lowest point in the landscape constructed by the cost function.

The annealing algorithm is inspired by the annealing in metallurgy and material science. It is a heat treatment that first heats up a material to a temperature at which recrystallisation occurs, and then cools it down again. Recrystalisation processes lower the free energy of the crystals [12]. It is an ancient technique to improve the properties of materials and make them more workable.

Following this process, simulated annealing is an optimisation method for approximating the global minimum of a given function. In simulated annealing, the system starts from a high energy state and by lowering the temperature very slowly, the system is expected to end up in the lowest energy state or at least a close approximation. However, there are two situations which may turn simulated annealing into an inefficient algorithm. First, if the landscape is too rugged and the energy barrier around local minima is too high, the system may get stuck in one of the local minima which is apparently not the optimal solution. These deep barriers may trap the system for a very long time during the evolution. The second problem is the complexity. The number of the candidate solutions usually grows exponentially with the problem size, but simulated annealing can only go through one configuration at a time. Unless there is a gradient that can guide the system towards the global minimum from any point of the configuration space, the simulated annealing algorithm can do no better than a random search.

On the other hand, quantum annealing may become more efficient and perform better than simulated annealing when facing these two situations, because the phenomenon of quantum tunnelling helps to explore the search space. More precisely, quantum mechanics allows the system to tunnel through very high barriers in a classically inaccessible path once barriers are narrow enough. Furthermore, if the Hamiltonian of a given problem is applied properly to the system, the quantum mechanical wave function can delocalise over the whole search space, that is, it has the ability to see the entire landscape during annealing [13]. In contrast, simulated annealing can only search the configuration space randomly and escape from local minima by the aid of thermal fluctuations. Therefore, quantum annealing when implemented on a quantum annealer may be superior to simu-

lated annealing in these two aspects. However, empirically quantum annealing does not always improve the search process and it has its own limitations. Some counter cases have been observed for k-SAT problems [14]. In brief, although for both algorithms the system may stop evolving at a local minimum state instead of the global minimum, if the barrier constraining the local minimum is narrow enough, the quantum tunnelling can give the system a chance to tunnel through the barrier and keep evolving towards the true minimum. An illustration is shown in Figure.1.

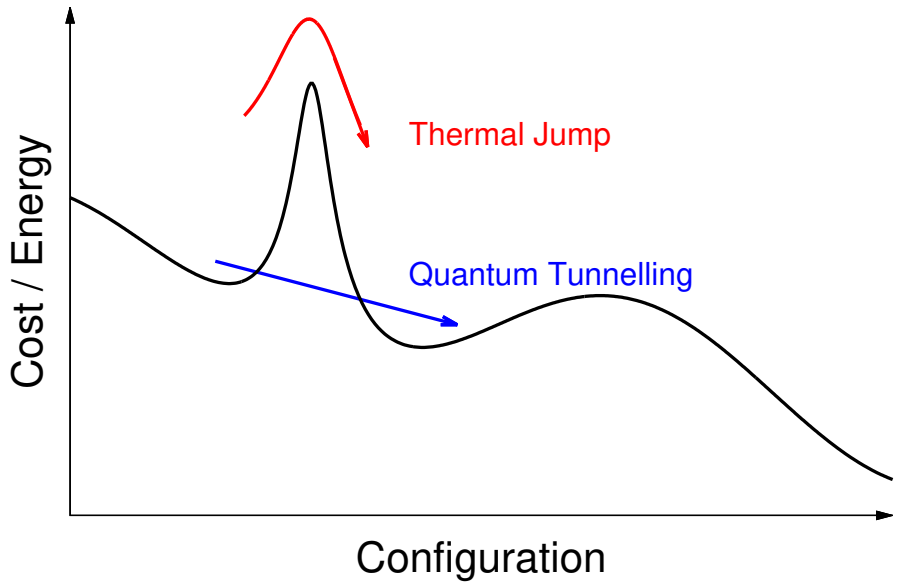

Figure 1: The difference between quantum annealing and simulated annealing.

In contrast to thermal fluctuations used in simulated annealing, the main feature of the quantum annealing process are quantum fluctuations. To bring in quantum fluctuations, a strong transverse field is applied and the system is prepared in the ground state of this Hamiltonian at the beginning of the quantum annealing process. During the annealing, the transverse field is slowly turned off while the problem Hamiltonian is slowly turned on. If this procedure progresses slowly enough, the system will stay still in the ground state. At the end of the quantum annealing process, the transverse field is complete switched off and the system should have evolved to the ground state of the problem Hamiltonian that encodes the given optimisation problem.

The Ising model is broadly used in statistical physics to study phase transitions. The model describes a set of lattice sites with discrete variables that represent the atomic spins being either up ($|\uparrow\rangle$) or down ($|\downarrow\rangle$). The three components of the spin operators when applying to the Hilbert space spanned by $|\uparrow\rangle$ and $|\downarrow\rangle$ are defined as

$$\sigma^x = \begin{pmatrix} 0 & 1 \\ 1 & 0 \end{pmatrix}, \sigma^y = \begin{pmatrix} 0 & -i \\ i & 0 \end{pmatrix}, \sigma^z = \begin{pmatrix} 1 & 0 \\ 0 & -1 \end{pmatrix}. \tag{1}$$

Please note that $|\uparrow\rangle$ and $|\downarrow\rangle$ are the eigenstates of σ^z with eigenvalues 1 and -1 respectively. The model Hamiltonian can be written as

$$H = -\sum_{i,j}^{N} \sum_{\alpha=x,y,z} J_{ij}^{\alpha} \sigma_i^{\alpha} \sigma_j^{\alpha} - \sum_{i}^{N} \sum_{\alpha=x,y,z} h_i^{\alpha} \sigma_i^{\alpha}, \tag{2}$$

which allows interaction between neighbours with evolution strength J_{ij}. If $J_{ij} > 0$, the interaction is called ferromagnetic and the neighbour spins have a higher probability to align parallel. In contrast, if $J_{ij} < 0$, it is antiferromagnetic and the neighbour spins favour opposite states. An external field h_i interacts with each spin. The spin tends to have positive direction when $h_i > 0$, and negative direction when $h_i < 0$. Obviously, finding the spin configuration of the ground state given a parameter set is the main difficult task after mapping an optimisation problem into the Hamiltonian.

The Hamiltonian used in the quantum annealing process can be written as

$$\begin{aligned} H(t) &= (1 - \frac{t}{T}) H_{init} + (\frac{t}{T}) H_{problem} \\ H_{init} &= -\sum_{i=1}^{N} h_i^x \sigma_i^x \\ H_{problem} &= -\sum_{i,j}^{N} J_{ij}^z \sigma_i^z \sigma_j^z - \sum_{i}^{N} h_i^z \sigma_i^z, \end{aligned} \tag{3}$$

where t is the current time step and T is total annealing time. It should be noted that by using $\left(1 - \frac{t}{T}\right)$ and $\left(\frac{t}{T}\right)$ as the time factors for H_{init} and $H_{problem}$ respectively in Eq. (3), it implies that the annealing proceeds with a linear time scheme. There are more general annealing schemes that can be implemented for the annealing process rather than a linear one. For the sake of simplicity, the linear annealing scheme is applied in the annealing process in this report. An illustration is shown in Figure 2.

The key feature of H_{init} is that it should be straightforward to construct and that its ground state is easy to find. With this chosen H_{init}, the ground state is

$$|x_1 = \uparrow\rangle |x_2 = \uparrow\rangle |x_3 = \uparrow\rangle \ldots |x_N = \uparrow\rangle, \tag{4}$$

where $|x_i = \uparrow\rangle$ denotes the eigenstate of σ_i^x. This state can be rewritten in a superposition of all 2^N basis eigenstates of σ_i^z,

$$\sum_{2^N} \frac{1}{\sqrt{2^N}} |z_1 = \uparrow,\downarrow\rangle |z_2 = \uparrow,\downarrow\rangle \ldots |z_N = \uparrow,\downarrow\rangle. \tag{5}$$

To summarise, the quantum annealing starts evolving with the system initialised in the ground state of H_{init}. According to the adiabatic theorem, which is introduced in section 2.2, if the total annealing time is long enough, the system can evolve adiabatically and remain in the ground state. As a result, when $H(t)$ shifts from H_{init} to $H_{problem}$ at the end

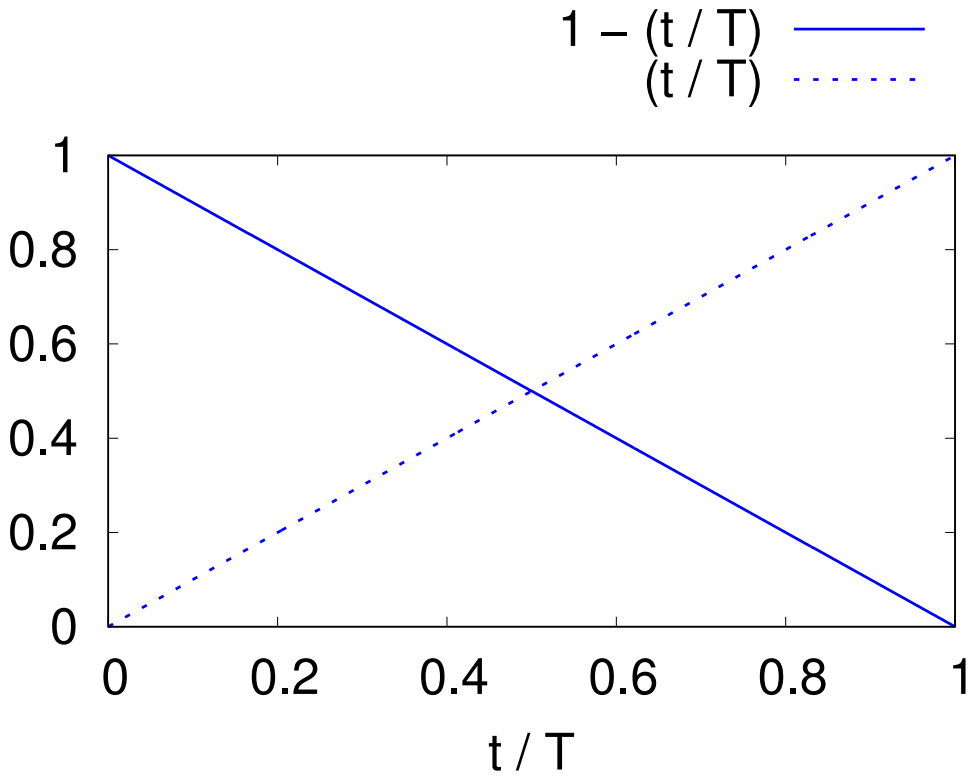

Figure 2: A linear annealing scheme for an annealing process of duration T.

of the annealing process, the system is expected to lie in the ground state of $H_{problem}$.

The quantum annealing algorithm is presented as follows [9, 15]:

Quantum Annealing Algorithm

1. Set up $H_{problem}$ according to a given problem. Combine H_{init} and $H_{problem}$ to build $H(t)$.

2. Initialise the system in the ground state of H_{init}. The ground state of H_{init} is designed in a way that it is simple to construct.

3. Evolve the system by solving the time-dependent Schrödinger equation for time t according for a given annealing scheme.

4. The system will end up in the ground state of $H_{problem}$, if the total annealing T is long enough.

It is worthwhile to mention the inherent difference between simulated annealing and quantum annealing. In the ideal case, simulated annealing has some random factor when choosing the starting point and also during the process, but quantum annealing does not

have this randomness. Therefore, in principal, quantum annealing will either always find the solution, or never, which leads to a bimodal distribution. Conversely, simulated annealing starting from a random state may have a uni-modal result. This is considered as a main criterion to distinguish between simulated annealing and quantum annealing [16]. Based on this, D-wave Systems Inc. declared that their quantum annealer has quantum characteristics, but some claimed that the same behaviour can be shown by a classical model [10].

2.2 Adiabatic Theorem

The adiabatic theorem mainly serves as the basis of quantum annealing. The concept is that if the Hamiltonian of an eigenstate alters gradually, then the state will remain an eigenstate at later times while the eigenenergy evolves continuously. The relation between a gradually varying Hamiltonian and adiabatic behaviour can be demonstrated as follows [17]: The time-dependent Schrödinger equation with $\hbar = 1$ is written as

$$i\frac{\partial |\psi(t)\rangle}{\partial t} = H(t)\,|\psi(t)\rangle\,, \tag{6}$$

where $H(t)$ is the time-dependent Hamiltonian and $|\psi(t)\rangle$ is a quantum state. Assume that the spectrum of $H(t)$ is nondegenerate. As a result, a basis can be defined as

$$H(t)\,|n(t)\rangle = E_n(t)\,|n(t)\rangle\,, \tag{7}$$

where $|n(t)\rangle$ is the set of eigenvectors chosen to be orthonormal. Suppose that the time-dependent Hamiltonian can be diagonalised by a unitary transformation

$$H_D(t) = U^{-1}(t)H(t)U(t), \tag{8}$$

where $H_D(t)$ stands for the diagonalised Hamiltonian and $U(t)$ is a unitary transformation that diagonalises the Hamiltonian $H(t)$. By multiplying U^{-1} to Eq. (6) from the left, it yields

$$iU^{-1}(t)\frac{\partial |\psi(t)\rangle}{\partial t} = U^{-1}H(t)\,|\psi(t)\rangle\,. \tag{9}$$

The right hand side of Eq. (9) can be transformed by using Eq. (8) as follows:

$$\begin{aligned} U^{-1}(t)H(t) &= H_D(t)U^{-1}(t), \\ U^{-1}(t)H(t)\,|\psi(t)\rangle &= H_D(t)U^{-1}(t)\,|\psi(t)\rangle = H_D(t)\,|\psi(t)\rangle_D\,, \end{aligned} \tag{10}$$

where $|\psi(t)\rangle_D \equiv U^{-1}\,|\psi(t)\rangle$ is the state of the system in the basis of eigenvectors of $H_D(t)$. The left hand side of Eq. (9) can be transformed as follows based on the integration by parts,

$$
\begin{aligned}
i\frac{\partial U^{-1}(t)\,|\psi(t)\rangle}{\partial t} &= i\frac{\partial U^{-1}(t)}{\partial t}\,|\psi(t)\rangle + iU^{-1}(t)\frac{\partial\,|\psi(t)\rangle}{\partial t},\\
iU^{-1}(t)\frac{\partial\,|\psi(t)\rangle}{\partial t} &= i\frac{\partial\,|\psi(t)\rangle_D}{\partial t} - i\frac{\partial U^{-1}(t)}{\partial t}\,|\psi(t)\rangle\,.
\end{aligned}
\tag{11}
$$

Combining Eq. (10) and Eq. (11), Eq. (9) can be rewritten as

$$
i\frac{\partial\,|\psi(t)\rangle_D}{\partial t} - i\frac{\partial U^{-1}}{\partial t}\,|\psi(t)\rangle = H_D\,|\psi(t)\rangle_D\,. \tag{12}
$$

If $H(t)$ changes sufficiently slow, $\partial H(t)/\partial t$ approaches zero. Thus, the unitary transformation, $U(t)$, and its inverse, $U^{-1}(t)$ are assumed to be slowly varying operators, which leads to

$$
i\frac{\partial\,|\psi(t)\rangle_D}{\partial t} = H_D(t)\,|\psi(t)\rangle_D\,. \tag{13}
$$

Consequently, the system can evolve separately in each energy eigenstate, because $H_D(t)$ is diagonal. In other words, this assures that, with a sufficiently slowly varying Hamiltonian, if the quantum system is in an instantaneous eigenstate of $H(t)$ at a certain point in time, it will remain in this eigenstate at all times.

2.3 Landau-Zener Transition

According to the Landau-Zener formula, another constraint on the quantum annealing process is the distance between the ground state energy and the first excited state energy. The Landau-Zener formula gives the probability of a diabatic transition from a lower energy eigenstate to a higher energy eigenstate. Although the adiabatic theorem implies that no diabatic transition will occur if $H(t)$ in Eq. (3) could vary infinitely slow, this is not the case for real systems with a finite annealing time. Once the system evolves in a finite annealing time from a lower energy eigenstate, the probability of finding the system in a higher energy state in the future can be determined by the Landau-Zener formula.

If $P_{adiabatic}$ is the probability of the system remaining in the ground state and evolving adiabatically and $P_{diabatic}$ is the probability for a diabatic transition, the relation between these two is $P_{adiabatic} = 1 - P_{diabatic}$. According to the Landau-Zener formula, $P_{diabatic}$ is given by

$$
P_{diabatic}(T) = \exp\!\left(-c\cdot\Delta_{min}^2\,T\right), \tag{14}
$$

where c is a constant, T is the total annealing time, and Δ_{min} is the minimum gap between two energy eigenstates during the annealing process, which is always referred to the gap between the ground state energy and the first excited state energy in this report. An illustration of the minimum gap can be found in Figure. 3.

The probability of a successful quantum annealing process is thus confined by the minimum gap Δ_{min} and the annealing time T correspondingly. The relation between the successful probability and Δ_{min} can be investigated for a fixed annealing time T. Simulation results are presented in Section 5 and Section 6.

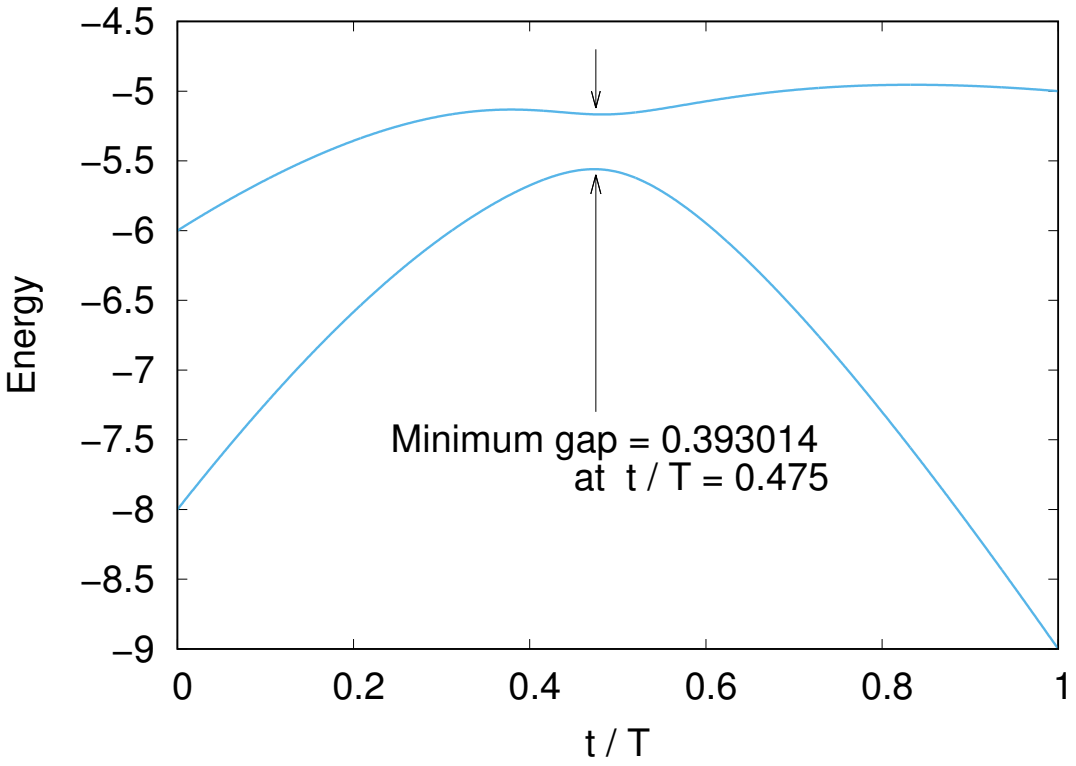

Figure 3: Two lowest energy states of the energy spectrum showing the minimum gap between the ground state energy and the first excited state energy during a quantum annealing process of duration T.

3 Optimisation Problems

3.1 Combinatorial Optimisation

If one needs to find the best choice among all available options, the problem can be considered as a combinatorial optimisation problem. Some practical examples are the travelling salesman problem, the closure problem and the assignment problem. Take the travelling salesman problem for instance: there are N cities located randomly in a given area and the goal is to plan a trip to visit every city once in the shortest travel distance. A straightforward approach is to try out all permutations and find the shortest path. The run time for this brute-force search is of the order of $N!$, which means that it grows as the factorial of the number of cities and the search space easily becomes too large for this approach to be feasible even for relatively small N ($N \sim 30$) [18].

Combinatorial optimisation can usually be cast into a problem of minimising a given cost function $H(S_1, S_2, S_3, \ldots S_N)$ with respect to N variables S_1, S_2, ... S_N, where the values of S_i with $i = 1, \cdots N$ belong to a finite discrete set [13]. The aim is to determine a configuration of values for the variables that yield the minimum value of the cost function. Combinatorial optimisation often has the following properties. The optimal solution is searched from a finite set of candidate solutions. The set of candidate solutions is discrete. Brute-force search is usually not feasible. Besides, even some problems with continuous variables can be reduced to combinatorial optimisation [19].

In the field of computer science, the complexity of a computational task is classified by the run time needed by the fastest algorithm relative to the size of the task. If a given task can be solved in polynomial time by using polynomially bound resources on a classical computer, it is considered to be in the class P. Although a P problem does not necessary means an easy problem, a polynomial bound on the evaluation time implies its difficulty will not grow exponentially with the problem size. Unfortunately, not all cases fall in this class, and some of the important ones fall outside, like the travelling salesman problem mentioned above.

A given task is said to be in the class NP, if the solution can be found in polynomial time by a non-deterministic Turing machine. A deterministic Turing machine can only perform one action for a given situation according to its set of rules, while a non-deterministic Turing machine can perform more than one action for a given situation and if any of them finds the solution, it achieves its goal. In other words, a non-deterministic Turing machine has the potential to explore exponentially many paths in parallel with time and check if any of them can solve the task. It is clear that a deterministic Turing machine is a weak version of a non-deterministic one. Therefore, the class P is also included inside the class NP as a special case. Not like a problem in the class P, for which a polynomial-time algorithm is known to exist, problems in the class NP are believed to require super-polynomial time.

There is a subset inside the class NP called NP-complete, which is considered to be

the hardest set among the class NP and all NP problems can be reduced into the class NP-complete with a polynomial overhead. It is generally believed that if one can find a polynomial algorithm to solve a NP-complete problem, all problems in the class NP can also be solved by this polynomial algorithm. The tasks that fall inside either the class NP or the class NP-complete are considered to be hard, because a non-deterministic Turing machine cannot yet be simulated by a deterministic Turing machine without an exponential growth of execution time.

Indeed there are algorithms that can solve some easy optimisation problems in polynomial time. For harder cases like the one belonging to the class NP-complete, although one cannot find the exact solution in polynomial time, there exists some specialised algorithms that can approximate the solution in a polynomial time. The downside is that these algorithms are very problem specific, which means a success in one NP-complete problem does not ensure the success when attacking other NP problems by using the same algorithm.

3.2 Boolean Satisfiability Problems

The Boolean satisfiability problem, abbreviated as the SAT problem, is a task of checking whether a given Boolean formula can be satisfied. To be more specific, the goal here is to find a configuration of true or false values for all variables in a given Boolean formula so that the final evaluation of the formula is true. The formula is called satisfiable when this configuration exists. On the other hand, the formula is not satisfiable, if the evaluation is false for all possible configurations.

The k-SAT problem with $k > 2$ has been proven to be in the class NP-complete, which implies that no algorithm can efficiently solve SAT problems in polynomial time. The parameter k defines the upper limit of the number of variables in one clause. An example is

$$(x_1 \vee x_2 \vee x_3) \wedge (x_4 \vee x_5 \vee \neg x_6),$$

where $\wedge$,$\vee$, and $\neg$ state for logical and, logical or, and logical not respectively. This is a Boolean formula in 3-SAT form, which has two clauses and each clause consists of 3 variables. This formula is satisfiable because the final evaluation is true if one of the variables x_1, x_2, x_3 is true in the first clause, and one of the variables $x_4, x_5, \neg x_6$ is true in the second clause.

In this report, 2-SAT problems are investigated. In contrast to those more general ones which are known to be NP-complete, the 2-SAT problem can be solved in polynomial time. A detail that should be mentioned is that the 2-SAT problems studied in this work all have only one unique configuration which leads to a true evaluation.

3.3 Mapping the 2-SAT Problem to the Ising Hamiltonian

A 2-SAT problem can only be solved by quantum annealing when its Boolean formula is mapped to an Ising Hamiltonian. The following simple example demonstrates how a Boolean formula is mapped on the Ising Hamiltonian. Consider the Boolean formula,

$$(x_1 \vee x_2) \wedge (x_3 \vee \neg x_4).$$

The first clause is true, when either x_1 or x_2 is true. The second clause is true, when x_3 is true or x_4 is false. The whole statement is true only when the evaluations of the both clauses are true. The aim is to cast the Boolean variables of this sample problem to the Ising variables. One possible way of mapping is as follows:

2-SAT Variables

	T	T	T	F
x_1	1	1	0	0
x_2	1	0	1	0

$\Rightarrow$

Ising variables

	T	T	T	F
σ_1	1	1	-1	-1
σ_2	1	-1	1	-1
$m = \sigma_1 + \sigma_2$	2	0	0	-2

	T	T	T	F
x_3	1	1	0	0
x_4	0	1	0	1

$\Rightarrow$

	T	T	T	F
σ_3	1	1	-1	-1
σ_4	-1	1	-1	1
$m = \sigma_3 - \sigma_4$	2	0	0	-2

Table 1: Mapping a 2-SAT problem in term of the Ising variables by using the transformation $\sigma_1 = 2x_i - 1$.

In order to encode the solution of the 2-SAT problem into the ground state of the Ising Hamiltonian, an Ising Hamiltonian can be written down with a variable m. Take the first clause for example, it yields

$$\begin{aligned} H &= m \cdot (m-2) \\ &= \sigma_1^2 + \sigma_2^2 + 2\sigma_1\sigma_2 - 2\sigma_1 - 2\sigma_2 \\ &= 2\sigma_1\sigma_2 - 2\sigma_1 - 2\sigma_2 + const. \end{aligned} \tag{15}$$

By comparing Eq. (15) with $H_{problem}$ of the Hamiltonian given in Eq. (3), one finds that h_1^z, h_2^z, and J_{12} correspond to 2, 2, and -2 respectively. The same procedure can be repeated for all clauses. After mapping, the original 2-SAT problem is ready to be solved with quantum annealing, because the ground state of the problem Hamiltonian can be transformed back to the solution of the original 2-SAT problem.

4 Simulation Algorithms

4.1 The Time-Dependent Schrödinger Equation and the Quantum Spin System

The quantum annealing process can be described in terms of the time-dependent Schrödinger equation, and thus the final state of the system can be determined by solving the time-dependent Schrödinger equation. The solution of the time-dependent Schrödinger equation provided in Eq. (6) is

$$\begin{aligned}\Psi(t+\tau) &= U(t+\tau,t)\Psi(t) \\ &= \exp_+(-i\int_t^{t+\tau} H(t')dt')\Psi(t),\end{aligned} \tag{16}$$

where τ is the size of the time step, and $U(t+\tau,t)$ is a unitary matrix that transforms the wave function from t to $t+\tau$. In order to conduct a numerical computation and ensure the unitary of the evolution operator, time is discretised in small time steps and $H(t')$ is assumed to be piecewise constant within these time steps. The solution can be written as

$$\Psi(t+\tau) = \exp\Big(-iH(t+\frac{\tau}{2})\tau\Big)\Psi(t).$$

To preserve the accuracy of the numerical solution, the size of the time step should be small enough to keep $H(t')$ piecewise constant. However, if the size is too small, the run time of the simulation will be too long.

The wave function $|\Psi\rangle$ of an N-spin system is constructed as the superposition of the basis states of the N spins. Each single spin has two possible basis states, $|\uparrow\rangle$ or $|\downarrow\rangle$. For the sake of convenience, these two states are denoted as $|0\rangle$ or $|1\rangle$, respectively. The reason will be explained after presenting the expression of $|\Psi\rangle$. The relation between both notations is defined as

$$|\uparrow\rangle = |0\rangle\,,\ |\downarrow\rangle = |1\rangle\,. \tag{17}$$

Thus, a single spin state can be written as a superposition of theses two basis states,

$$|\Psi\rangle = a(0)\,|0\rangle + a(1)\,|1\rangle\,, \tag{18}$$

where $a(0)$ and $a(1)$ are the probability amplitudes of each basis state. Using the same representation, a N-spin system can be constructed with 2^N basis states and written as

$$\begin{aligned}|\Psi\rangle =& a(00\ldots0)\,|00\ldots0\rangle + a(00\ldots1)\,|00\ldots1\rangle + \ldots \\ &+ a(11\ldots0)\,|11\ldots0\rangle + a(11\ldots1)\,|11\ldots1\rangle\,.\end{aligned} \tag{19}$$

The following equation should hold because of the normalisation requirement, $\langle\Psi|\Psi\rangle = 1$:

$$\sum_{\sigma_1,\sigma_2,\ldots,\sigma_N=|0\rangle,|1\rangle} |a(\sigma_1,\sigma_2,\ldots,\sigma_N)|^2 = 1. \tag{20}$$

One may notice that by using the notation with $|0\rangle$ and $|1\rangle$, the state in Eq. (19) is represented in binary number notation. With the binary number notation, the basis states can be read as integers ranging from 0 to $2^N - 1$. When comparing the simulation results with the known solution state, this notation makes the comparison simpler. In addition, it is easy to estimate the memory request to store the wave function in this notation. It immediately follows that the memory request scales exponentially with the number of spins, N.

Equation (3) shows that there are two kind of terms in the Hamiltonian, namely are the single spin term and the double spin term. When applying these terms to $|\Psi\rangle$, the computation can be reduced to a series of 2×2 and 4×4 in-place matrix computations instead of a computation of the entire $2^N \times 2^N$ matrix. After applying these two terms to the state, the state is written as follows:

$$\begin{aligned} |\Psi\rangle \to |\Psi'\rangle = a'(00\ldots0)\,|00\ldots0\rangle + a'(00\ldots1)\,|00\ldots1\rangle + \ldots \\ + a'(11\ldots0)\,|11\ldots0\rangle + a'(11\ldots1)\,|11\ldots1\rangle\,, \end{aligned} \tag{21}$$

where $\alpha = x, y, z$. If the operator is σ_i^x, it interchanges the state up and state down, which corresponds to a swap of a pair component of $|\Psi\rangle$. This leads to the following equation

$$\begin{aligned} a'(\bullet\cdots\bullet 0\bullet\cdots\bullet) &= +a(\bullet\cdots\bullet 1\bullet\cdots\bullet) \\ a'(\bullet\cdots\bullet 1\bullet\cdots\bullet) &= +a(\bullet\cdots\bullet 0\bullet\cdots\bullet), \end{aligned} \tag{22}$$

where the $\bullet$ is used to indicate that the bits on the corresponding position are the same. If the operator is σ_i^y, according to Eq. (1), the coefficients obey the relation

$$\begin{aligned} a'(\bullet\cdots\bullet 0\bullet\cdots\bullet) &= -ia(\bullet\cdots\bullet 1\bullet\cdots\bullet) \\ a'(\bullet\cdots\bullet 1\bullet\cdots\bullet) &= +ia(\bullet\cdots\bullet 0\bullet\cdots\bullet). \end{aligned} \tag{23}$$

Although Eq. (3) does not contain a σ_i^y component, σ_i^y will later be used in the case for finite temperature. If the operator is σ_i^z, it reverses the sign of all coefficients of $|\Psi\rangle$ for which the i^{th} bit of the vector has value 1, which yields

$$\begin{aligned} a'(\bullet\cdots\bullet 0\bullet\cdots\bullet) &= +a(\bullet\cdots\bullet 0\bullet\cdots\bullet) \\ a'(\bullet\cdots\bullet 1\bullet\cdots\bullet) &= -a(\bullet\cdots\bullet 1\bullet\cdots\bullet). \end{aligned} \tag{24}$$

Similarly, applying the two spin operator $\sigma_i^z\sigma_j^z$ to $|\Psi\rangle$ leads to a sign interchange between the coefficients of $|\Psi\rangle$ for which the i^{th} bit and the j^{th} bit of the vector have different values. Hence,

$$\begin{aligned} a'(\bullet\cdots\bullet 0\bullet\cdots\bullet 0\bullet\cdots\bullet) &= +a(\bullet\cdots\bullet 0\bullet\cdots\bullet 0\bullet\cdots\bullet) \\ a'(\bullet\cdots\bullet 1\bullet\cdots\bullet 0\bullet\cdots\bullet) &= -a(\bullet\cdots\bullet 1\bullet\cdots\bullet 0\bullet\cdots\bullet) \\ a'(\bullet\cdots\bullet 0\bullet\cdots\bullet 1\bullet\cdots\bullet) &= -a(\bullet\cdots\bullet 0\bullet\cdots\bullet 1\bullet\cdots\bullet) \\ a'(\bullet\cdots\bullet 1\bullet\cdots\bullet 1\bullet\cdots\bullet) &= +a(\bullet\cdots\bullet 1\bullet\cdots\bullet 1\bullet\cdots\bullet). \end{aligned} \tag{25}$$

It is worth mentioning again that the operations mentioned here are done in place. Namely, instead of creating and using an extra unnecessary vector, these operations only manipulate the necessary component in the state vector $|\Psi\rangle$. Thus, $|\Psi'\rangle = H|\Psi\rangle$ can be calculated efficiently. This approach serves as the basis of the algorithms introduced in the following subsections.

4.2 Algorithms for a System at Zero Temperature

4.2.1 The Full Diagonalisation Method

Based on the fact that the Hamiltonian H is a Hermitian operator formed by a $2^N \times 2^N$ matrix, it has a complete set of eigenstates and eigenvalues. This implies that the Hamiltonian H can be transformed into a diagonal matrix Λ spanned by its eigenvalues and the unitary matrix V composed of its eigenstates. The transformation is given by $H = V\Lambda V^\dagger$. Thus, the time evolution can be calculated as $U(\tau) = \exp(-i\tau H) = V\exp(-i\tau\Lambda)V^\dagger$. If V and Λ can be obtained by diagonalising H, the time evolution becomes a series of matrix multiplications. Since diagonalisation is a classic matrix transformation, standard software libraries can be used.

The elements of H can be computed by repeatedly applying the Hamiltonian H to the basis vector $|i\rangle$, which results in $|i'\rangle = H|i\rangle$. The $|i'\rangle$ is the column of H in matrix form. In more detail, $|i\rangle$ is firstly assigned to be $(1,0,\ldots,0)^T$. $|i'\rangle = H|i\rangle$ will then result in the first column of the matrix H. The same calculation for $(0,1,0,\ldots,0)^T$ will lead to the second column of the matrix H and so forth. Consequently, the elements of the matrix H can be determined.

The main drawback of this approach is the limitation on scaling. While diagonalising the matrix H, the memory request and the run time of the standard algorithm scale as D^2 and D^3 ($D = 2^N$) respectively. Due to the exponential growth of the matrix size D, the full diagonalisation method can only be used for a quantum system of small size. Therefore, this approach serves mostly as a tool to validate the correctness of other algorithms for solving the time-dependent Schrödinger equation.

4.2.2 The Suzuki-Trotter Product Formula Approach

The Suzuki-Trotter product formula approach can reduce the memory request and the run time when dealing with a larger quantum system [20]. The main idea is that a unitary matrix exponential can be approximated by decomposing it properly into matrix exponentials with small matrix size,

$$
\begin{aligned}
U(t) &= \exp(-itH) \\
&= \exp(-it(H_1 + H_2 + \cdots + H_K)) \\
&= \lim_{m\to\infty} (\prod_{k=1}^{K} \exp(-itH_k/m))^m.
\end{aligned}
\tag{26}
$$

If the size of the time step is sufficiently small, a good approximation of $U(t)$ suggested by Eq. (26) is

$$
\tilde{U}_1(\tau) = \exp(-i\tau H_1)\exp(-i\tau H_2)\ldots\exp(-i\tau H_K), \tag{27}
$$

where $\tau = t/m$ is the size of the time step. The Taylor series of $U(t)$ and $\tilde{U}_1(t = m\tau) = \tilde{U}_1(\tau)^m$ are identical up to first order in τ. Thus $\tilde{U}_1(t)$ is the first order approximation of $U(t)$. Furthermore, if all H_i in Eq. (27) are Hermitian, $\tilde{U}_1(t)$ is unitary by construction. Consequently, the algorithm based on Eq. (27) will be unconditionally stable. The accuracy of the algorithm can be increased by using the second order approximation and it yields

$$
\begin{aligned}
\tilde{U}_2(\tau) &= \tilde{U}_1(\frac{\tau}{2})^T \tilde{U}_1(\frac{\tau}{2}) \\
&= \exp\left(\frac{-i\tau H_K}{2}\right)\exp\left(\frac{-i\tau H_{K-1}}{2}\right)\ldots\exp\left(\frac{-i\tau H_1}{2}\right)\exp\left(\frac{-i\tau H_1}{2}\right)\ldots\exp\left(\frac{-i\tau H_K}{2}\right).
\end{aligned}
\tag{28}
$$

$\tilde{U}_2(\tau)$ is also unitary by construction. For a fixed accuracy in this $\tilde{U}_2(\tau)$ approximation, the amount of memory required and the run time scale in the order of D ($D = 2^N$). The crucial step in this algorithm is to choose H_k properly so that the calculation of their matrix exponentials is simple and efficient.

Based on the Hamiltonian given in Eq. (3), one efficient way to construct a second order approximation is

$$
\begin{aligned}
\tilde{U}(\tau) = \exp\left(\frac{-i\tau H_{\sigma_\alpha}}{2}\right)\exp\left(\frac{-i\tau H_{\sigma_x\sigma_x}}{2}\right)\exp\left(\frac{-i\tau H_{\sigma_y\sigma_y}}{2}\right)\exp\left(-i\tau H_{\sigma_z\sigma_z}\right) \\
\exp\left(\frac{-i\tau H_{\sigma_y\sigma_y}}{2}\right)\exp\left(\frac{-i\tau H_{\sigma_x\sigma_x}}{2}\right)\exp\left(\frac{-i\tau H_{\sigma_\alpha}}{2}\right)
\end{aligned}
\tag{29}
$$

with

$$\exp\left(\frac{-i\tau H_{\sigma_\alpha}}{2}\right) = \exp\left(\frac{-i\tau\left(-\sum_{i=1}^{N}\sum_{\alpha=x,y,z} h_i^\alpha \sigma_i^\alpha\right)}{2}\right), \tag{30}$$

$$\exp\left(\frac{-i\tau H_{\sigma_x\sigma_x}}{2}\right) = \exp\left(\frac{-i\tau\left(-\sum_{i,j=1}^{N} J_{ij}^x \sigma_i^x \sigma_j^x\right)}{2}\right), \tag{31}$$

$$\exp\left(\frac{-i\tau H_{\sigma_y\sigma_y}}{2}\right) = \exp\left(\frac{-i\tau\left(-\sum_{i,j=1}^{N} J_{ij}^y \sigma_i^y \sigma_j^y\right)}{2}\right), \tag{32}$$

$$\exp\left(-i\tau H_{\sigma_z\sigma_z}\right) = \exp\left(-i\tau\left(-\sum_{i,j=1}^{N} J_{ij}^z \sigma_i^z \sigma_j^z\right)\right). \tag{33}$$

The reason why decomposing in this way is that the analytical expression of each matrix exponential is known. First, Eq. (30) can be rewritten as

$$\exp\left(\frac{-i\tau(-\sum_{i=1}^{N}\sum_{\alpha=x,y,z} h_i^\alpha \sigma_i^\alpha)}{2}\right) = \prod_{i=1}^{N} \exp\left(\frac{i\tau\sum_{\alpha=x,y,z} h_i^\alpha \sigma_i^\alpha}{2}\right). \tag{34}$$

With the aid of the following equation, which denotes the rotation of the vector σ about the vector $\mathbf{v}$

$$\exp(i\mathbf{v}\cdot\sigma) = \mathbb{I}\cos(v) + \frac{i\mathbf{v}\cdot\sigma}{v}\sin(v), \tag{35}$$

where v is the norm of $\mathbf{v}$, the matrix exponential of Eq. (34) can be written as

$$\exp\left(\frac{i\tau\sum_{\alpha=x,y,z} h_i^\alpha \sigma_i^\alpha}{2}\right) = \begin{pmatrix} \cos\frac{\tau h_i}{2} + \frac{ih_i^z}{h_i}\sin\frac{\tau h_i}{2} & \frac{ih_i^x + h_i^y}{h_i}\sin\frac{\tau h_i}{2} \\ \frac{ih_i^x - h_i^y}{h_i}\sin\frac{\tau h_i}{2} & \cos\frac{\tau h_i}{2} - \frac{ih_i^z}{h_i}\sin\frac{\tau h_i}{2} \end{pmatrix}, \tag{36}$$

where h_i is the norm of the vector $\mathbf{h}_i = (h_i^x, h_i^y, h_i^z)$. It can be concluded from Eq. (36), that the calculation of the time evolution for single spin terms becomes a series of 2×2 matrix calculations. In addition, this calculation can be done by picking right pairs of corresponding states and applying Eq. (36).

For the case of the double spin operator, since the spin operators with different labels commute, Eq. (31), Eq. (32), and Eq. (33) can be decomposed into

$$\exp\left(\frac{-i\tau\left(-\sum_{i,j=1}^{N} J_{ij}^{x}\sigma_i^x\sigma_j^x\right)}{2}\right) = \prod_{i,j=1}^{N}\exp\left(\frac{i\tau J_{i,j}^{x}\sigma_i^x\sigma_j^x}{2}\right), \tag{37}$$

$$\exp\left(\frac{-i\tau\left(-\sum_{i,j=1}^{N} J_{ij}^{y}\sigma_i^y\sigma_j^y\right)}{2}\right) = \prod_{i,j=1}^{N}\exp\left(\frac{i\tau J_{i,j}^{y}\sigma_i^y\sigma_j^y}{2}\right), \tag{38}$$

$$\exp\left(-i\tau\left(-\sum_{i,j=1}^{N} J_{ij}^{z}\sigma_i^z\sigma_j^z\right)\right) = \prod_{i,j=1}^{N}\exp\left(i\tau J_{i,j}^{z}\sigma_i^z\sigma_j^z\right). \tag{39}$$

The above expressions, likewise, can be determined analytically and yield

$$\exp\left(\frac{i\tau J_{i,j}^{x}\sigma_i^x\sigma_j^x}{2}\right) = \begin{pmatrix} \cos\left(\frac{J_{i,j}^{x}\tau}{2}\right) & 0 & 0 & i\sin\left(\frac{J_{i,j}^{x}\tau}{2}\right) \\ 0 & \cos\left(\frac{J_{i,j}^{x}\tau}{2}\right) & i\sin\left(\frac{J_{i,j}^{x}\tau}{2}\right) & 0 \\ 0 & i\sin\left(\frac{J_{i,j}^{x}\tau}{2}\right) & \cos\left(\frac{J_{i,j}^{x}\tau}{2}\right) & 0 \\ i\sin\left(\frac{J_{i,j}^{x}\tau}{2}\right) & 0 & 0 & \cos\left(\frac{J_{i,j}^{x}\tau}{2}\right) \end{pmatrix}, \tag{40}$$

$$\exp\left(\frac{i\tau J_{i,j}^{y}\sigma_i^y\sigma_j^y}{2}\right) = \begin{pmatrix} \cos\left(-\frac{J_{i,j}^{y}\tau}{2}\right) & 0 & 0 & i\sin\left(-\frac{J_{i,j}^{y}\tau}{2}\right) \\ 0 & \cos\left(\frac{J_{i,j}^{y}\tau}{2}\right) & i\sin\left(\frac{J_{i,j}^{y}\tau}{2}\right) & 0 \\ 0 & i\sin\left(\frac{J_{i,j}^{y}\tau}{2}\right) & \cos\left(\frac{J_{i,j}^{y}\tau}{2}\right) & 0 \\ i\sin\left(-\frac{J_{i,j}^{y}\tau}{2}\right) & 0 & 0 & \cos\left(-\frac{J_{i,j}^{y}\tau}{2}\right) \end{pmatrix}, \tag{41}$$

$$\exp\left(i\tau J_{i,j}^{z}\sigma_i^z\sigma_j^z\right) = \begin{pmatrix} \exp\left(iJ_{i,j}^{z}\tau\right) & 0 & 0 & 0 \\ 0 & \exp\left(-iJ_{i,j}^{z}\tau\right) & 0 & 0 \\ 0 & 0 & \exp\left(-iJ_{i,j}^{z}\tau\right) & 0 \\ 0 & 0 & 0 & \exp\left(iJ_{i,j}^{z}\tau\right) \end{pmatrix}. \tag{42}$$

In a similar way, the calculation of the time evolution of double spin operators can be evaluated by picking the 4 corresponding states. Moreover, with these analytical expressions (i.e. Eq. (36), Eq. (40), Eq. (41), and Eq. (42)), it is now possible to carry out $\tilde{U}(\tau)$ in Eq. (29) and apply it to $|\Psi(t)\rangle$. Thus, the time evolution of the wave function can be calculated.

These two algorithms, the full diagonalisation method and the Suzuki-Trotter Product Formula approach are sufficient to simulate a quantum annealer at zero temperature, namely in ideal condition, on a classical computer. Nevertheless, in order to simulate a quantum annealer at finite temperature, the temperature should be introduced by coupling

with a heat bath and the computation process will be more complicated.

4.3 Algorithms for a System at Finite Temperature

4.3.1 Canonical Ensemble

In order to simulate a system at finite temperature, the quantum subsystem S is coupled to a heat bath B and the Hamiltonian of the entire system (i.e. S+B) is defined as

$$H = H_S + H_B + gH_{SB}, \tag{43}$$

where H_S is the Hamiltonian of the system, H_B is the Hamiltonian of the heat bath, and H_{SB} is the Hamiltonian describing the interaction between the system S and the heat bath B with g indicating the global coupling strength between S and B.

After coupling a heat bath to the system, the entire system can no longer be described by a pure state. Instead, the entire system should be considered as a mixed state constructed by statistically combining certain pure states. The heat bath can be represented with a canonical ensemble, $\rho_B = e^{-\beta H_B}/Z$ with $Z = \sum_B e^{-\beta H_B}$ is the canonical partition function and β is the inverse temperature, in which the energy is not known but the temperature is specified. Let A be an observable. The expectation value of A can then be written as

$$\langle A(t)\rangle = \mathbf{Tr}\left(\rho_B \rho_S A(t)\right) = \sum_B \frac{e^{-\beta E_B}}{Z} \langle E_B| \langle S| e^{iHt} A e^{-iHt} |S\rangle |E_B\rangle, \tag{44}$$

where $|E_B\rangle$ are the microstates of the heat bath with energy E_B, and $\rho_S = |S\rangle\langle S|$. Equation (44) can be rewritten as

$$\langle A(t)\rangle = \sum_B \frac{e^{-\beta E_B}}{Z} \langle \Psi(t)| A |\Psi(t)\rangle, \tag{45}$$

where $|\Psi\rangle = e^{-iHt}|S\rangle|E_B\rangle$. This form implies that the core part of the simulation of an isolated system and of a system coupled with a heat bath is similar. The only difference between them is that, for the latter case, the simulation needs to be repeated over all possible microstates of the heat bath and assembled with the corresponding probability distribution. Hence, the run time grows exponentially with the size of the heat bath. This property makes the canonical ensemble approach unpractical when dealing with a large heat bath, although this approach can well describe the entire system.

4.3.2 The Random Sampling Method

The exponential scaling behaviour of the run time of the canonical ensemble approach limits its application to a heat bath with small size. The random sampling method presented here does not have this behaviour, which makes it a proper method when the size

of the heat bath is large. The random sampling method relies on the hypothesis that, when solving the time-dependent Schrödinger equation, the exact result can be approximated by solving it with a set of samples of random initial states [21]. In order to show this approximation works, Eq. (44) is rewritten in any orthonormal basis $|B_i\rangle$ as

$$\langle A(t)\rangle = \mathbf{Tr}\left(\rho_B \rho_S A(t)\right) = \sum_{n=1}^{N_B} \langle B_n| \langle S| \frac{e^{-\beta H_B/2}}{\sqrt{Z}} e^{iHt} A e^{-iHt} \frac{e^{-\beta H_B/2}}{\sqrt{Z}} |S\rangle |B_n\rangle , \tag{46}$$

where N_B is the dimension of the Hilbert space of the heat bath. A random state $|\phi\rangle$ can be constructed by complex random numbers, c_n, of which the mean is 0. It yields

$$|\phi\rangle = \sum_{n=1}^{N_B} c_n |S\rangle |B_n\rangle , \quad \text{with} \quad c_n \equiv f_n + i g_n. \tag{47}$$

A projection of $\frac{e^{-\beta H_B/2}}{\sqrt{Z}}$ on $|\phi\rangle$ can be introduced, which yields

$$\left|\phi'\right\rangle = \sum_{n=1}^{N_B} c_n \frac{e^{-\beta H_B/2}}{\sqrt{Z}} |S\rangle |B_n\rangle . \tag{48}$$

The expectation value of $A(t)$ with respect to $|\phi'\rangle$ is give by

$$\left\langle \phi'\right| A(t) \left|\phi'\right\rangle = \sum_{m,n=1}^{N_B} c_m^\star c_n \langle B_m| \langle S| \frac{e^{-\beta H_B/2}}{\sqrt{Z}} e^{iHt} A e^{-iHt} \frac{e^{-\beta H_B/2}}{\sqrt{Z}} |S\rangle |B_n\rangle . \tag{49}$$

If K realisations of the random initial states are sampled, the result becomes

$$\frac{1}{K}\sum_{p=1}^{K} \left\langle \phi'_p\right| A(t) \left|\phi'_p\right\rangle = \frac{1}{K}\sum_{p=1}^{K}\sum_{m,n=1}^{N_B} c_{m,p}^\star c_{n,p} \langle B_m| \langle S| \frac{e^{-\beta H_B/2}}{\sqrt{Z}} e^{iHt} A e^{-iHt} \frac{e^{-\beta H_B/2}}{\sqrt{Z}} |S\rangle |B_n\rangle . \tag{50}$$

If there is no correlation between the random coefficients in different realisations, and the random coefficients f_n and g_n are drawn from an even and symmetric probability distribution, the following statement can be made.

$$\lim_{K\to\infty} \frac{1}{K}\sum_{p=1}^{K} c_{m,p}^\star c_{n,p} = E(|c|^2)\delta_{m,n}, \tag{51}$$

where $E(\cdot)$ is the expectation value based on the probability distribution used to draw c_n. The subscript n and p of $c_{n,p}$ were removed because it does not depend on n and p. Putting this relation back to Eq. (50) leads to

$$\begin{aligned} \lim_{K\to\infty} \frac{1}{K}\sum_{p=1}^{K} \left\langle \phi'_p\right| A \left|\phi'_p\right\rangle &= E(|c|^2) \sum_{n=1}^{N_B} \langle B_n| \langle S| \frac{e^{-\beta H_B/2}}{\sqrt{Z}} e^{iHt} A e^{-iHt} \frac{e^{-\beta H_B/2}}{\sqrt{Z}} |S\rangle |B_n\rangle \\ &= E(|c|^2)\mathbf{Tr}\left(\rho_B \rho_S A\right). \end{aligned} \tag{52}$$

For a large but finite K, the statement is as follows:

$$\frac{1}{K}\sum_{p=1}^{K} c^{\star}_{m,p}c_{n,p} = E(|c|^2)\delta_{m,n} + O(\frac{1}{\sqrt{K}}). \tag{53}$$

This implies that the accuracy of the simulation can be improved by including more realisations. Furthermore, a strong result can be shown [21]. The statistical error is proportional to $1/\sqrt{KD}$, where D is the dimension of the Hilbert space of the heat bath. To summarise, the random sampling method suggests that the expectation value of an observable A can be computed by sampling over the projected random initial states $\left|\phi'_p\right\rangle$ based on the fact that the time evolution can be calculated efficiently by the Suzuki-Trotter product formula approach. In addition, the initial state $\left|\phi'_p\right\rangle$ can be prepared by the power method, $\left|\phi'_p\right\rangle \propto [1+\left(\frac{-\beta H_B}{2M}\right)]^M |\phi\rangle$ for a large M. The random sampling method can provide a statistically reliable result without repeating the calculation for all energy eigenstates of the heat bath.

5 Simulation Results for a Quantum Annealer at Zero Temperature

For the ideal case, the system consists of 8 spins. There is no heat bath coupled to the system. In other words, there is no temperature effect (ideal case). The time scheme of the annealing is the linear time scheme.

5.1 The Evolution of the Energy, the Success Probability, and the Spin Value

For the ideal case, the simulation methods used are the full diagonalisation method and the Suzuki-Trotter product formula approach. First, the result of the Suzuki-Trotter product formula approach is compared with the result of the full diagonalisation method in Figure 4, in order to validate the correctness of the result of the Suzuki-Trotter product formula approach. At the beginning of the annealing, the system is in the ground state of the initial Hamiltonian, so the success probability is low. During the annealing, the system slowly transits from the ground state of the initial Hamiltonian to the ground state of the problem Hamiltonian. As a result, the success probability proceeds towards 1 at the end of the annealing process.

The energy of the system is also an important observable to watch on during the annealing process. The result for a particular 2-SAT problem is shown in Figure 5. The system starts with an energy equal to -8, because it is in the ground state of H_{init}, which is $-\sum_{i=1}^{8} h_i^x \sigma_i^x$ for an 8 spin system. At the end of the annealing, the system is in the ground state of $H_{problem}$. In this particular case, the ground state energy of $H_{problem}$ is -9.

Another interesting observable is the spin value which is shown in Figure 6. In similar fashion, since the system starts from the ground state of H_{init}, the values of $\sigma_1^x, \sigma_2^x \cdots \sigma_8^x$ are 1. During the annealing, these values approach 0. On the other hand, the value of $\sigma_1^z, \sigma_2^z \cdots \sigma_8^z$ evolves from 0 towards the configuration of the ground state of $H_{problem}$.

To be brief, the result of the simulation indicates that a successful quantum annealing process can lead the system to the ground state of the problem Hamiltonian and let the spin value end up in the ground state configuration. According to the adiabatic theorem and the Landau-Zener formula, the total annealing time and the minimum gap may influence the quantum annealing process. The result of these effects will be shown in the following subsections.

5.2 The Effect of the Total Annealing Time

The adiabatic theorem requires a slowly varying Hamiltonian to make the system remain in the ground state while its eigenenergy evolves continuously. In other words, the total

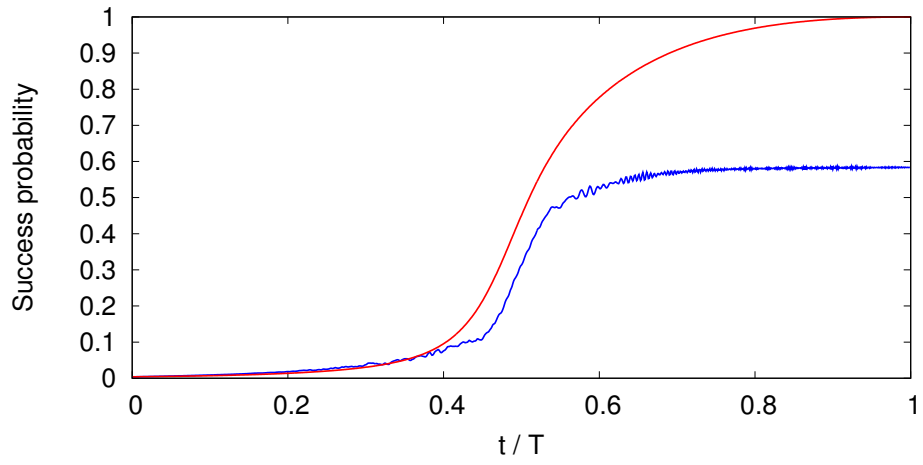

(a) $\tau = 1.0$

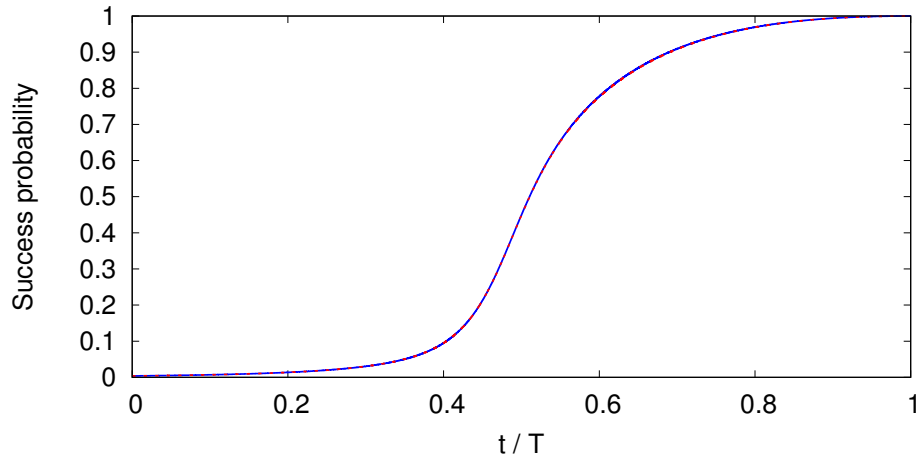

(b) $\tau = 0.1$

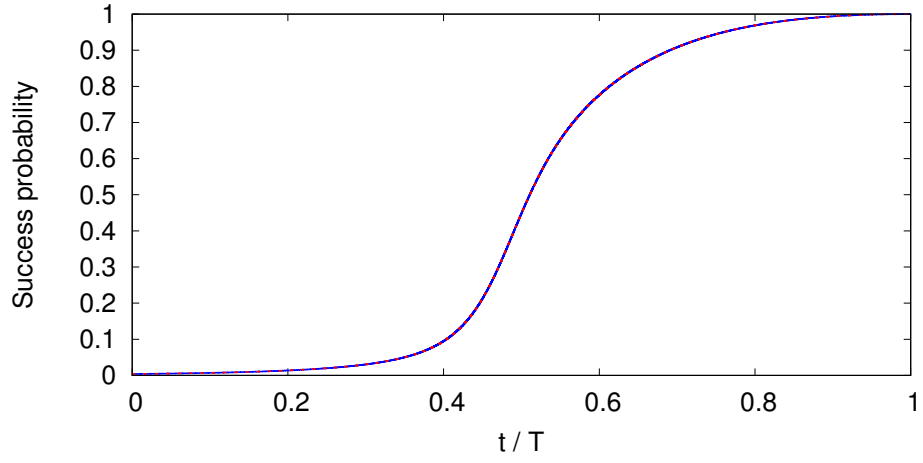

(c) $\tau = 0.01$

Figure 4: A comparison of the result simulated with the Suzuki-Trotter product formula approach (blue curve) and the result simulated with the full diaganolisaiton method (red curve) for the success probability as a function of the annealing time t/T for different time steps τ. The success probability is defined as the overlap of the current wave function with the wave function of the exact ground state, $\left\langle \Psi(t/T) \middle| \Psi_{gs} \right\rangle$.

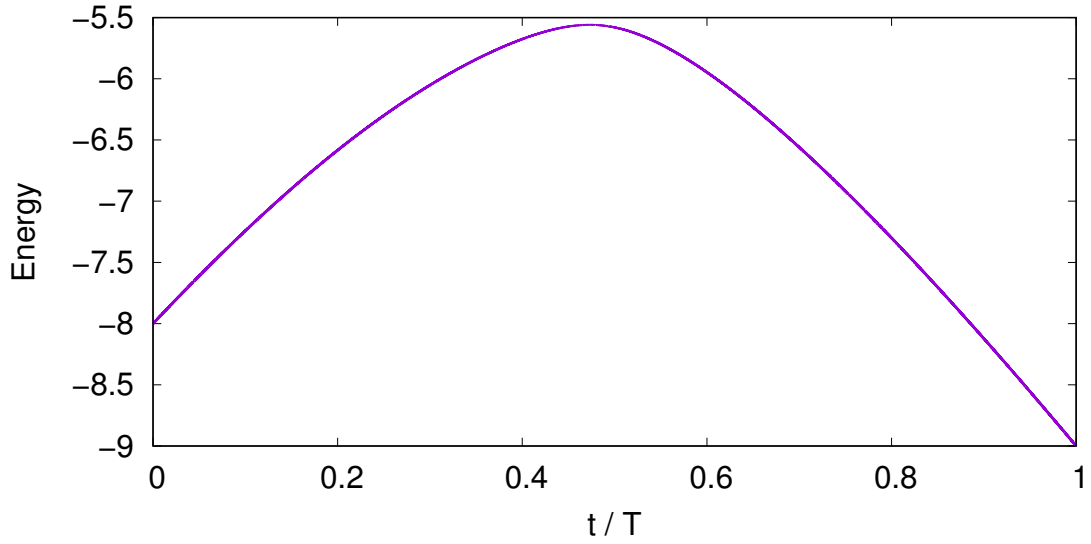

Figure 5: The energy evolution of an 8 spin system for a particular 2-SAT problem.

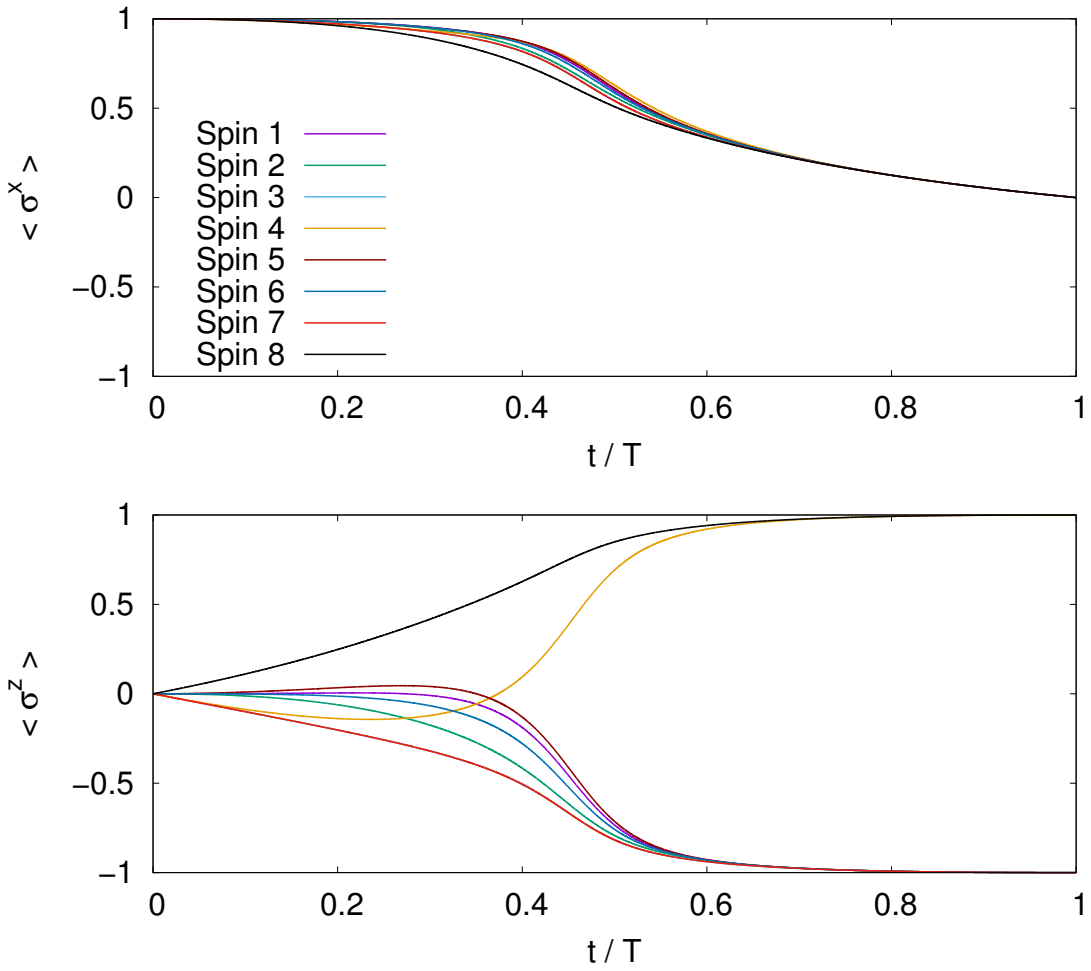

Figure 6: The evolution of the spin values for a particular 2-SAT problem.

annealing time should be long enough. When the total annealing time is not long enough, the success probability cannot reach 1 in the end. The effect of this is shown in Figure 7(*Top*). Besides, instead of tracking the ground state energy, the annealing path of the energy becomes gradually larger than the ground state energy, which indicates the system ends in a higher energy state. This effect is shown in Figure 7(*Bottom*).

5.3 The Effect of the Minimum Gap

It is known that the minimum gap influences the annealing according to the Landau-Zener formula. With Eq. (14), the success probability is expected to decrease when the minimum gap decreases. In Figure 8, an example energy spectrum of a particular 2-SAT problem with its minimum gap is shown.

In Figure 9, each cross point stands for the simulation result of a particular 2-SAT problem and in total 100 2-SAT problems are shown. The relation of the success probability as a function of the minimum gap does agree with what the Landau-Zener formula describes. Based on this result, it can be seen that the difficulty of a problem relies on the value of the minimum gap. If the minimum gap of a 2-SAT problem is small, the system may need a longer total annealing time to reach the ground state of the problem Hamiltonian.

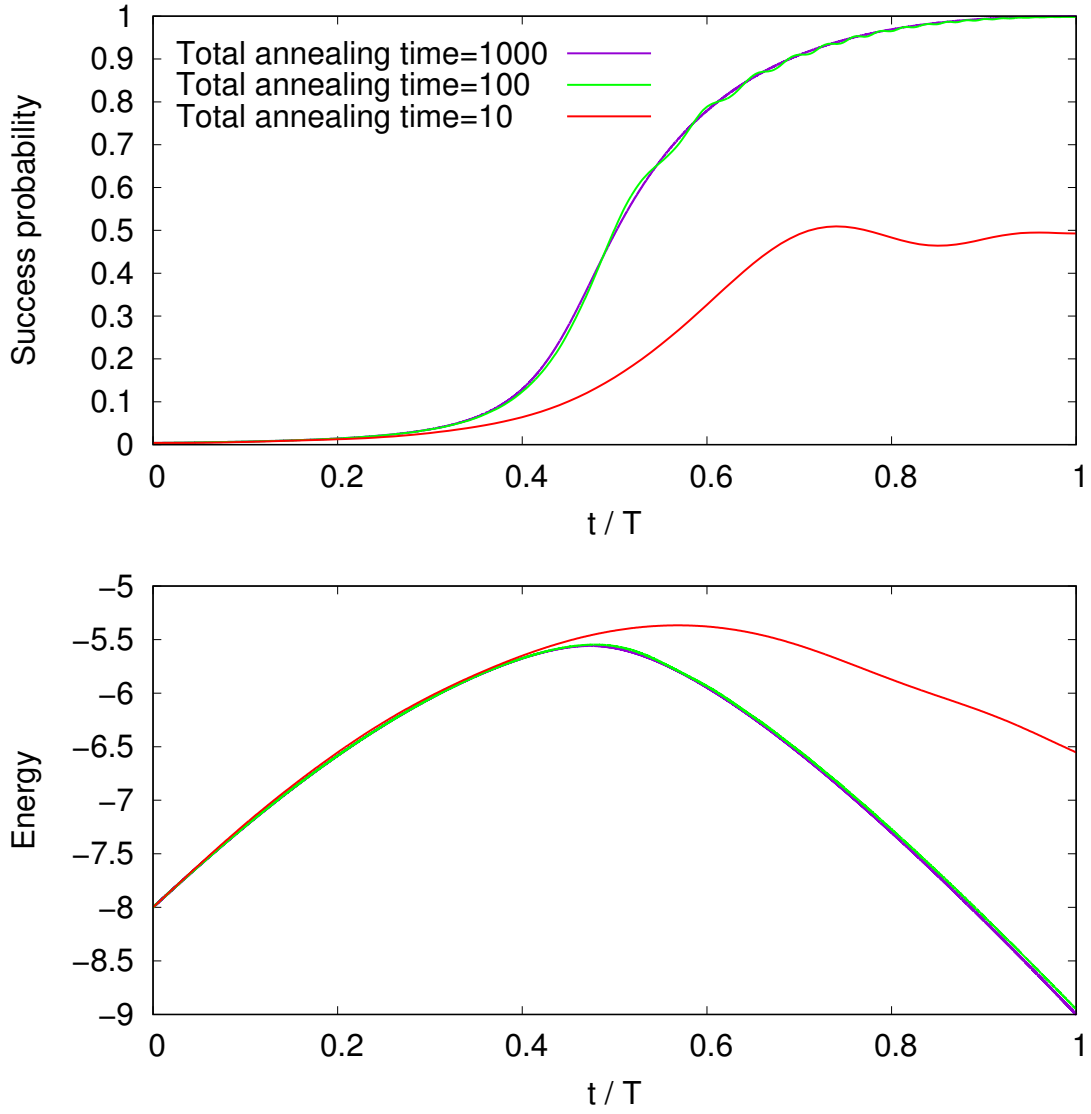

Figure 7: (*Top*) The evolution of the success probability for different total annealing times. (*Bottom*) The evolution of the energy for different total annealing times.

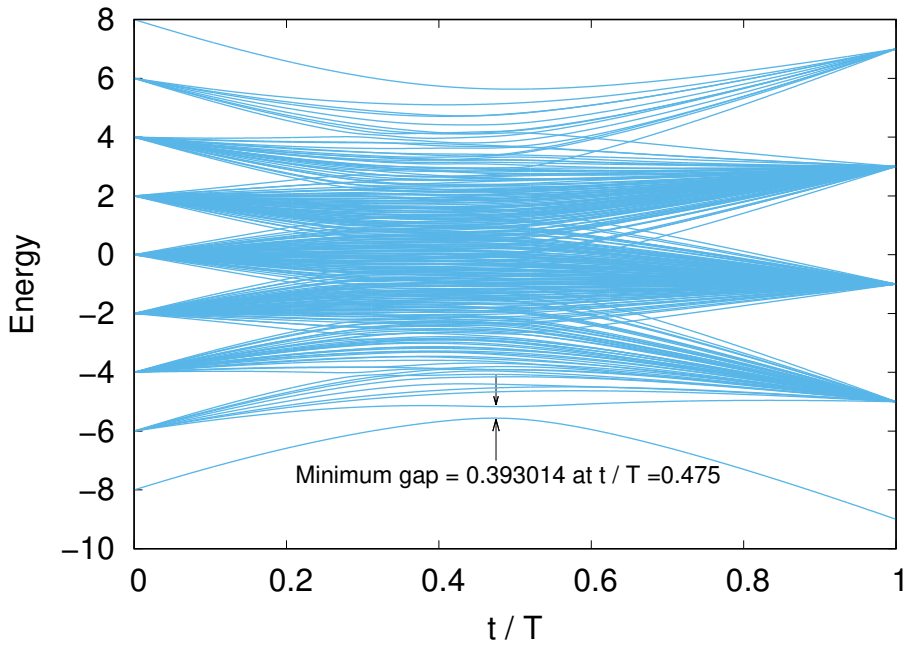

(a)

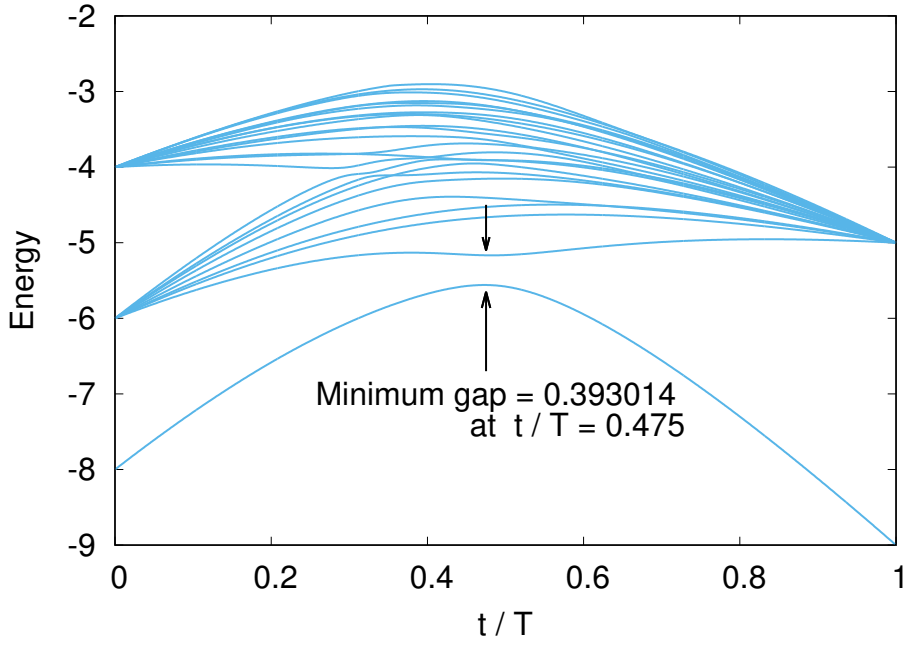

(b)

Figure 8: (a) The energy spectrum of a particular 2-SAT problem. The minimum gap between the ground state and the first excited state occurs at $t/T = 0.475$ with value $= 0.393014$. (b) A close look on the energy spectrum.

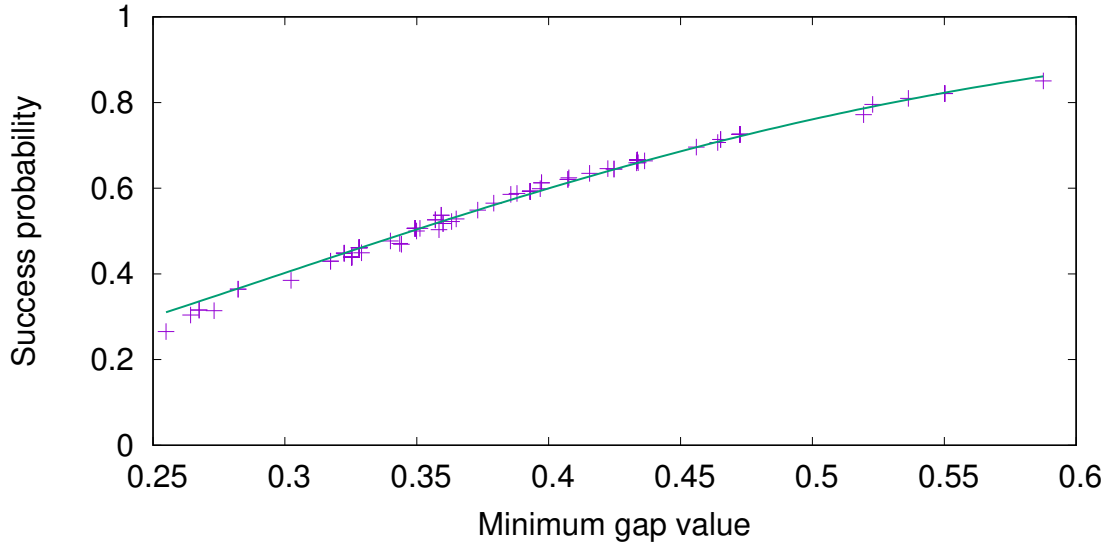

Figure 9: Success probability as a function of the minimum gap value for 100 different 2-SAT problems. The total annealing time of the simulation is 200. The green line is the fit of $P_{adiabatic} = 1 - \exp\left(-c' \cdot \Delta_{min}^2\right)$.

6 Simulation Results for a Quantum Annealer at Finite Temperature

In the previous section, the simulation results of the zero temperature (ideal) case has been presented. However, in the real world, the system is influenced by the environment. The main difference is the temperature. In the ideal case, the system is perfectly isolated from the environment and stays at zero temperature. On the other hand, in reality, the system evolves at finite temperature instead of zero temperature. The Hamiltonian of the entire system is constructed according to Eq. (43). The system and the heat bath contain both 8 spins for the presented simulation result.

6.1 Validation of the Random Sampling Method

In principal, the simulation of the entire system can be done with the Suzuki-Trotter product formula approach by approximating the heat bath with the canonical ensemble. However, when the size of the entire system increases, the run time of the simulation causes the simulation to become not practical. Consequently, the random sampling method is much more preferred in order to reduce the run time of the simulation. The comparison of the results of the random sampling method and the canonical ensemble approach is shown in Figure 10. Different colours indicate different coupling strengths. It is obvious that the result is not stable when using only one simulation run in the random sampling approach. If the simulation is repeated several times with different initial random wave functions, the average result becomes close to that of the canonical ensemble approach.

6.2 The Effect of the Temperature

A set of simulation results for different temperatures is shown in Figure 11. Based on this, some interpretations can be made. First, the purple line (g = 0.0) always stays the same across plots with different temperatures. The reason for this is the zero coupling strength between the system and the heat bath. That is, although the temperature of the heat bath raises from zero temperature to finite temperature, it cannot influence the system. The system is isolated from the environment, what corresponds to the ideal case. Second, the effect of finite temperature harms the annealing process for non-zero coupling strength. However, This effect does not uniformly reduce the success probability. Indeed, the overall success probability does decrease, but shows a trend of going up when the total annealing time is short, then going down, and going up again when the total annealing time is longer. A further detail of this effect is shown in Figure 12. It can be explained by the thermal equilibration process between the system and the heat bath [22]. When the total annealing time is short, the heat bath does not yet have enough time to influence the system and the system can stay in its coherent state. In this case, the way that the system evolves during the annealing process is similar to the way it evolves in the ideal case (zero temperature). As a result, the success probability increases when the total annealing time gets longer. After the total annealing time increases to a certain time, it

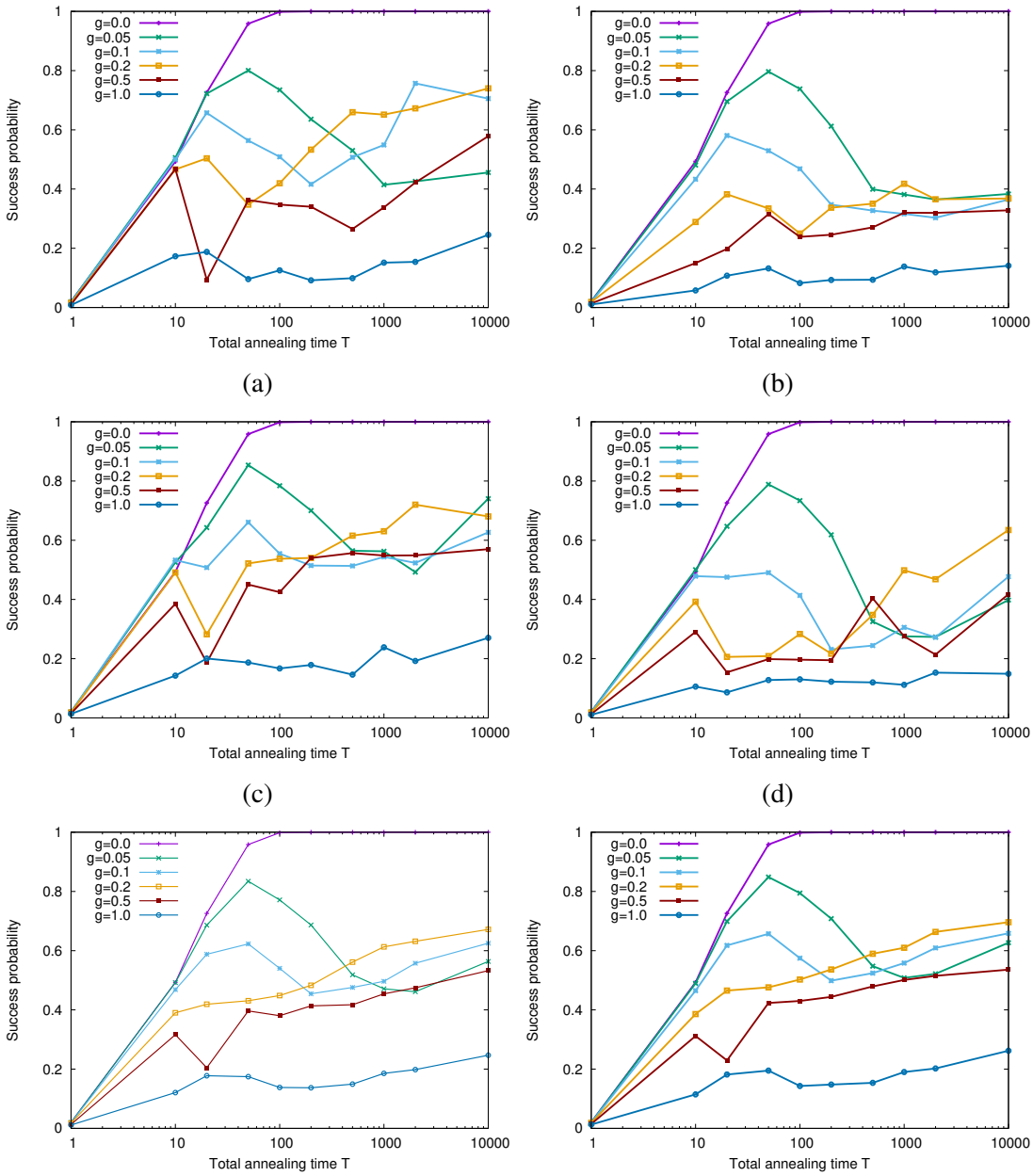

Figure 10: Success probability as a function of the total annealing time T for different coupling strengths g between the system and the heat bath. The temperature is set to 1. Plot (a), (b), (c), and (d) show the results of a single simulation run using the random sampling method. Plot (e) shows the average result of 12 runs using the random sampling method. Plot (f) depicts the simulation result done by computing all canonical ensemble states. It can be seen that Plot (e) and Plot (f) are similar.

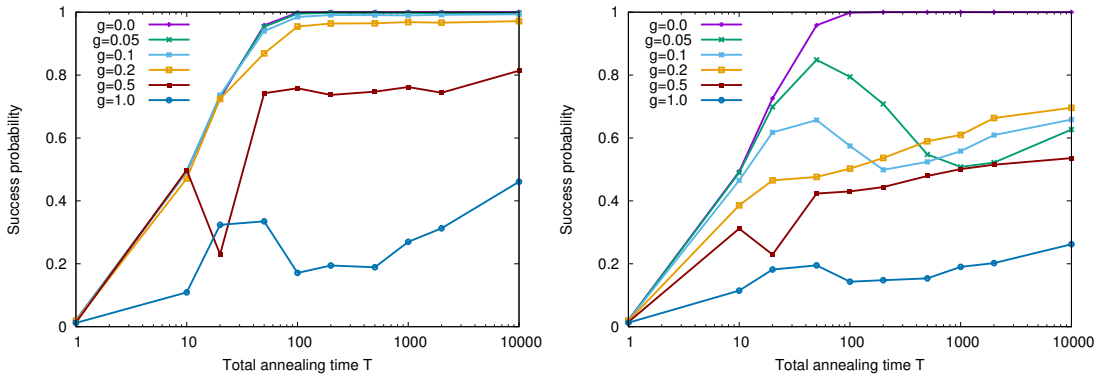

(a) Temperature = 0.02

(b) Temperature = 1

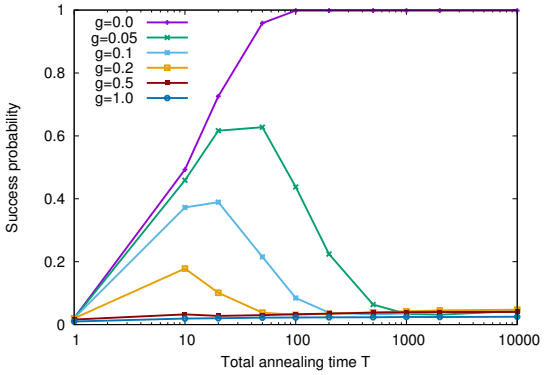

(c) Temperature = 1000

Figure 11: The simulation results of quantum annealing for different coupling strengths g between the system and the heat bath at different temperatures. The simulation is done with the canonical ensemble approach.

becomes sufficiently long for the heat bath to influence the system. Inside this regime, the heat bath starts to really interact with the system and harm the coherence of the system. The entire system enters a non-equilibrium state. Therefore, when the total annealing time increase, the success probability goes down. If the total annealing time gets even longer, the system and the heat bath will reach a quasi-static state. In other words, quantum annealing happens so slow that the system can be thermalised by the heat bath at each time. Therefore, the success probability becomes again larger with a longer total annealing time.

6.3 The Effect of the Minimum Gap

According to the Landau-Zener formula, the minimum gap has an influence on the difficulty of the annealing process. If the minimum gap is small, the annealing may need a longer total annealing time to keep the system in the ground state during the annealing process. In the ideal case, the simulation result can be fitted well with this model as shown in Figure 9. Following a similar set up, the simulation is done again but with a heat bath connected to the system. Since each instance is a 16 spin system (i.e. S = 8, B = 8) and in

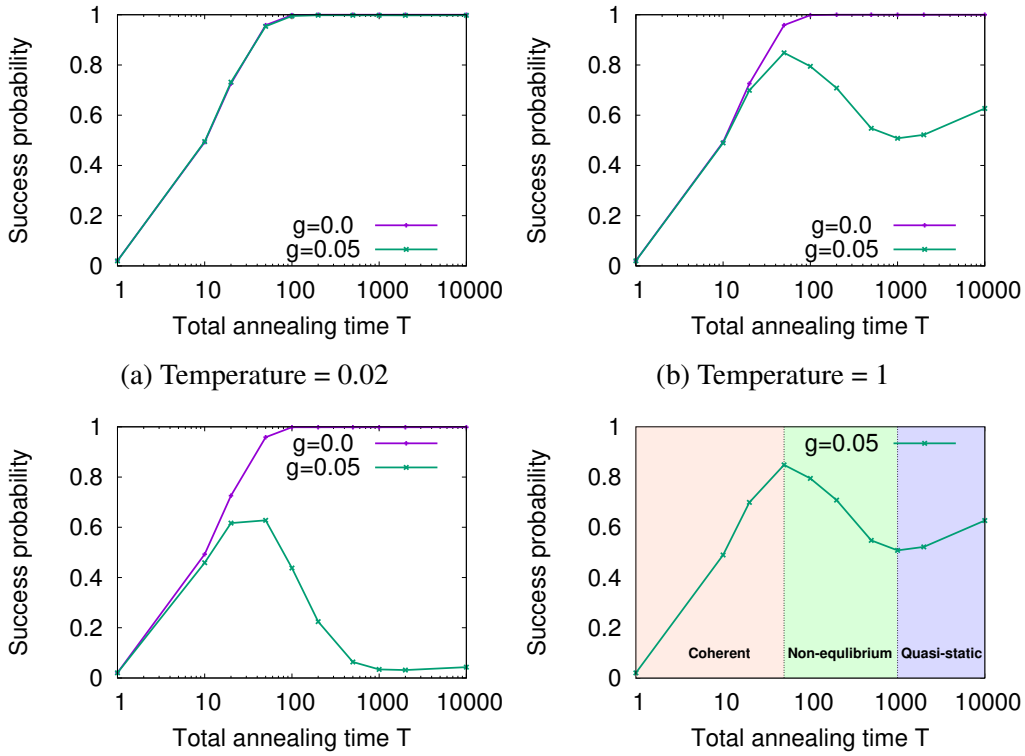

(a) Temperature = 0.02

(b) Temperature = 1

(c) Temperature = 1000

(d)

Figure 12: Success probability as a function of the total annealing time T for different coupling strengths g between the system and the heat bath and for different temperatures of the heat bath. In Figure (a) the temperature is low enough so that the heat bath is still in its ground state. So, the temperature effect does not influence the system much and both curves for different g are quite similar. By contrast, in Figure (c) the temperature is high. Consequently, the success probability becomes very low in the regime of non-equilibrium. In addition, it is hard for the success probability to go up again even when the entire system reaches a quasi-static state. In Figure (b) the heat bath is at a moderate temperature. The curve first goes up because the system is still in its coherent state. Then the curve goes down because of the influence of the heat bath. The curve goes up again when the entire system enters a quasi-static state. Figure (d) is an illustration that demonstrates the three different regions: coherent, non-equilibrium, and quasi-static. Similar simulation results of this behaviour are shown in [22].

total 100 2-SAT problems are involved, the algorithm used here is the random sampling method in order to reduce the run time of the simulation. The results are shown in Figure 13 and Figure 14.

In Figure 13, the plot with $g = 0.0$ corresponds to the result in the ideal condition, because there is no interaction between the system and the heat bath. If the coupling strength is turned on, the first effect is the drop of the success probability. It can be seen that when the success probability of the result with $g = 0.0$ climbs up to around 0.8, the success probability of the result with $g = 1.0$ stays only between 0 and 0.2. Second, the role of the coupling factor not only cuts down the success probability, but also causes scattering. For the results with $g = 0.0$, the data points almost form a smooth line, which is described by the Landau-Zener formula. By contrast, for the results with $g = 0.5$ the data points scatter in the range of 0 to 0.5. However, for the result with $g = 1.0$, the range of scattering becomes narrower. This can be understood as a combined effect of the above mentioned effects. The strong interaction between the system and the heat bath suppresses the growth of the success probability. Although a large coupling factor tends to enlarge the range of scattering, the range is made narrower because of the reduction of the overall success probability. As a result, the range of scattering for the results with $g = 1.0$ is narrower than that for the results with $g = 0.5$.

In Figure 14, a similar effect can be observed. For the results with temperature $= 0.01$, the success probability can raise to around 1. An increase of the temperature causes both the drop of the overall success probability and the scattering of the data points. The comparison of the results with temperature $= 0.5$ and the results with temperature $= 1.0$ also shows that a combined effect of both may narrow the range of the scattering instead of enlarging it. It is worth explaining why there is no much difference between the results with temperature $= 0.01$, the results with temperature $= 0.05$, and the results with temperature $= 0.1$. The reason is that, at these low temperatures, the heat bath is in its ground state for these three cases. Consequently, the result of these three simulations are similar.

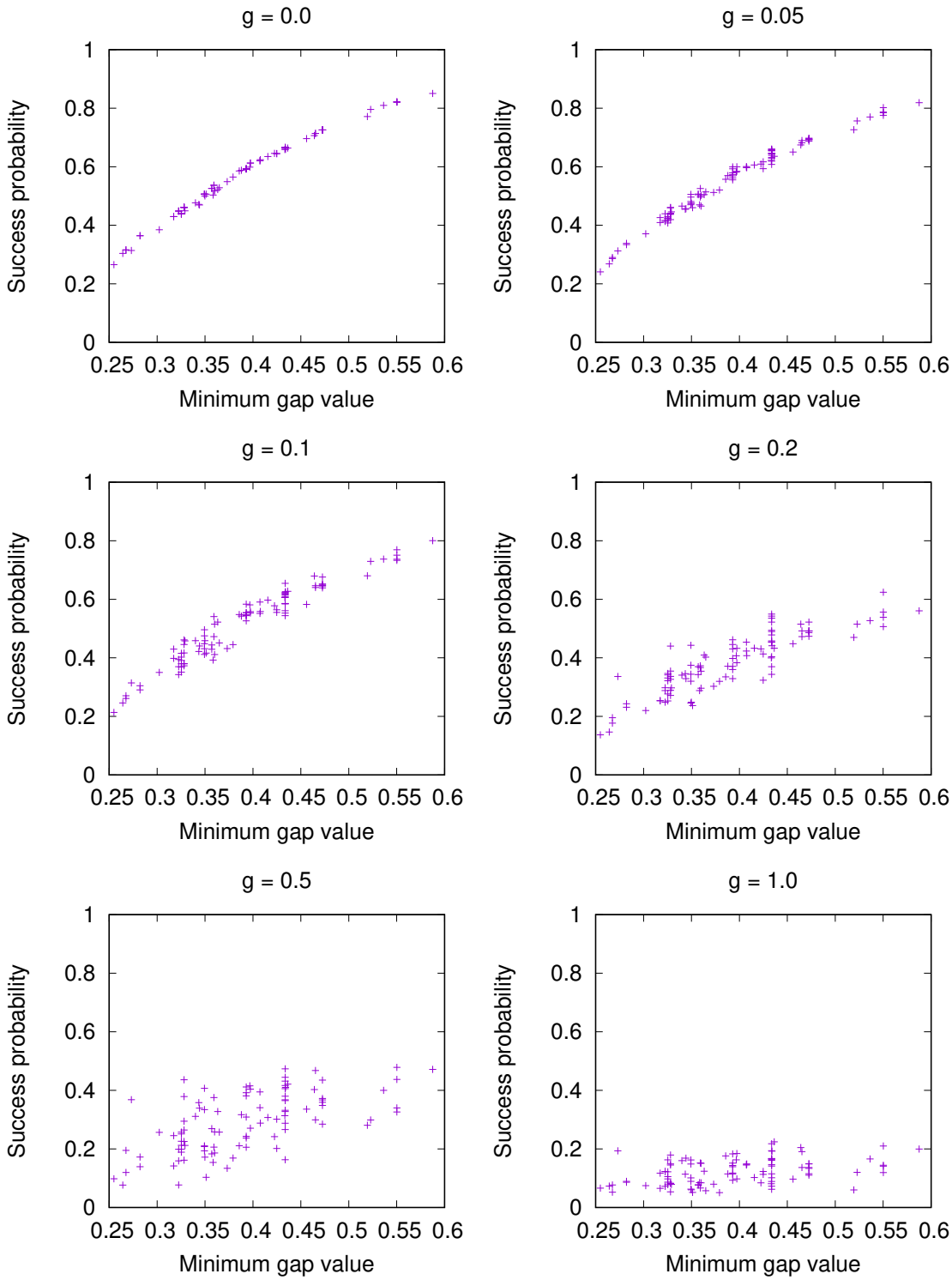

Figure 13: Simulation results for the success probability as a function of the minimum gap value for a set of 100 different 2-SAT problems for different values of the coupling strength g between the system and the heat bath. The total annealing time of the simulation is 200 and the temperature is 1.

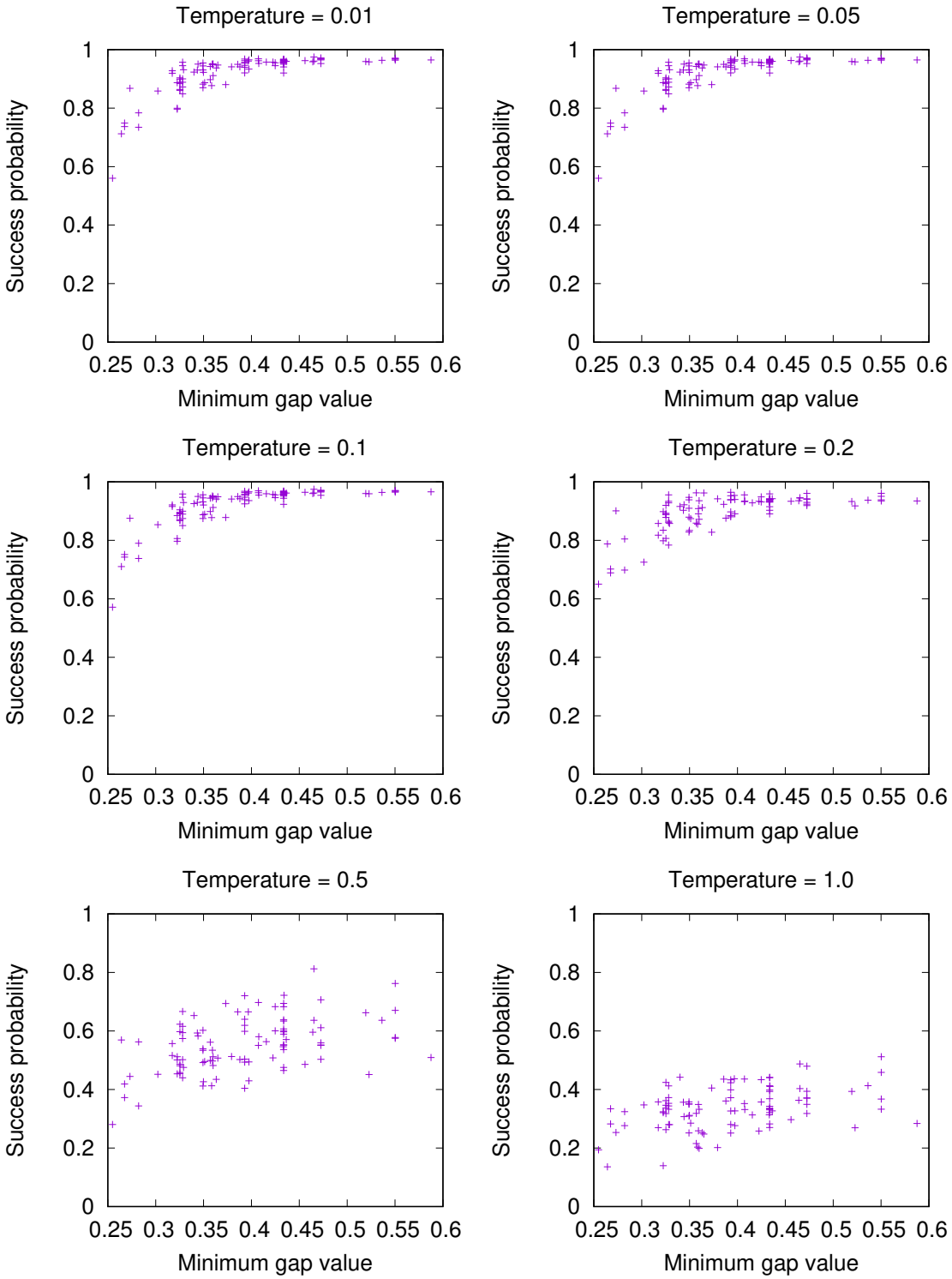

Figure 14: Simulation results for the success probability as a function of the minimum gap value for a set of 100 different 2-SAT problems for different values of the temperature of the heat bath. The total annealing time of the simulation is 1000 and the coupling factor is 0.2.

7 Applications on Machine Learning

The properties of quantum annealing when dealing with combinatorial optimisation makes it a potential candidate for machine learning applications. A tree cover detector based on aerial photography was implemented on a quantum annealer [23]. Boosting is the learning algorithm used in this application. The main idea of boosting is that a strong classifier can be constructed by properly combining a set of weak classifiers. A weak classifier is required to classify only slightly better than a random guess, which has a 50% correct rate. The critical part of boosting is to find proper weights for these weak classifiers and build a strong classifier. In order to implement the algorithm on a quantum annealer, the original boosting formula can be modified into the following one

$$C(t) = \text{sign}\left(\sum_{i=1}^{N} w_i c_i(t)\right), \tag{54}$$

where t is the data sample, $c_i \in \{-1,+1\}$ are the weak classifiers, and $w_i \in \{0,+1\}$ is the weight of the weak classifiers. The weights are required to be binary in this modified version. As a result, the strong classifier becomes just a majority vote of the weak classifiers. The cost function chosen here is the regulated quadratic loss function. With a set of training data, T, if each single data t has been classified correctly and labelled by $y(t) \in \{-1,+1\}$, the goal of the learning is

$$\arg\min_{w_i}\left\{\sum_{t\in T}\left(\sum_{i=1}^{N} w_i c_i(t) - y(t)\right)^2 + \lambda\sum_{i=1}^{N} w_i\right\}, \tag{55}$$

where λ is the regularisation parameter. The formula implies that if a weak classifier, $c_i(t)$, can in general give data the same label as $y(t)$ does, it is better to keep this weak classifier, which can be done by setting w_i equal to 1. On the other hand, if $c_i(t)$ cannot label the training data set correctly most of the time, this weak classifier should probably be discarded by setting w_i equal to 0. The role of the regularisation parameter is to prevent overfitting. That is, only the important weak classifiers are selected as part of the strong classifier. If the algorithm tries to include more weak classifiers than what it actually needs, the regularisation parameter will penalise this behaviour by raising up the cost value. This formula can be rewritten as follows by expanding quadratic part,

$$\arg\min_{w_i}\left\{\sum_{i}\left(\lambda - 2\sum_{t\in T} c_i(t)y(t)\right)w_i + \sum_{i,j}\left(\sum_{t\in T} c_i(t)c_j(t)\right)w_i w_j + const\right\}. \tag{56}$$

The form of the argument is similar to the optimisation problem that can be solved by a quantum annealer. However, the quantum annealing algorithm prefers variables w_i to be in a set of $\{-1,+1\}$ instead of $\{0,+1\}$. A variable transformation can be made by assigning $s_i = 2w_i - 1$ with $s_i \in \{-1,+1\}$ and the formula becomes

$$\arg\min_{s_i} \left\{ \sum_i \left(\frac{\lambda}{2} - \sum_{t\in T} c_i(t)y(t) + \frac{1}{2}\sum_j \left(\sum_{t\in T} c_i(t)c_j(t) \right) \right) s_i + \frac{1}{2}\sum_{i>j} \left(\sum_{t\in T} c_i(t)c_j(t) \right) s_i s_j \right\}. \tag{57}$$

With this proper form, the quantum annealer can step in and solve the optimisation problem. One can also simply require w_i to be in a set of $\{-1,+1\}$ in Eq. (55), but there is no corresponding regularisation part to prevent the algorithm from overfitting. The performance of these two forms depends on the applications and their empirical data.

The second application is a feature extraction of the human face implemented on a quantum annealer [24]. The aim of a feature extraction is to transform a large set of raw data into a reduced set of informative and non-redundant features. In order to implement this with a quantum annealer processor, nonnegative binary matrix factorisation (NBMF) is used. NBMF can be described as follows.

$$V^{n\times m} \approx W^{n\times k} H^{k\times m}, \tag{58}$$

where n is the dimension of the data, m is the number of the data, k is the number of the feature extracted and $k < n$. The matrix elements of W must be nonnegative and the matrix elements of H must be binary. The goal of the learning is

$$\arg\min_{H} \|V - WH\|_F, \tag{59}$$

where $\|\cdot\|_F$ is the Frobenius norm. This formula can be decomposed into a set of independent optimisation problems based on each column of H, because i^{th} column of WH only depends only on the i^{th} column of H and other columns of H do not have any impact on this at all. Therefore Eq. (59) can be simplified into a series of the following equations for $i = 1,2,\cdots,m$,

$$H_i = \arg\min_{\mathbf{q}} \|V_i - W\mathbf{q}\|_2, \tag{60}$$

where H_i denotes the i^{th} column of H and V_i denotes the i^{th} column of V. In order to solve this linear least squares problem with a quantum annealer, a further transformation can be made and it results in

$$\arg\min_{q_i} \left\{ \sum_i^k \left(\sum_r^n V_r W_{ir} \right) q_i + \sum_{i,j}^k \left(\sum_r^n W_{ir}^T W_{rj} \right) q_i q_j + const \right\}, \tag{61}$$

where q_i denotes the i^{th} element of $\mathbf{q}$. Although, with this form, q_i will be solved in a set of $\{-1,+1\}$ by a quantum annealer rather than the required binary set $\{0,+1\}$, a feature extraction can still be constructed. One can reform the formula by substituting variable $s_i = 2q_i - 1$ as in the previous example and make the final configuration of s_i in $\{-1,+1\}$. The performance of these two forms again can only be benchmarked with empirical data.

As the two examples showed above, the quantum annealing technique can be considered as a different computational approach when implementing some machine learning algorithms. However, there are some drawbacks. First, the original algorithm needs to be transformed into a form of combinatorial optimisation that can be solved by a quantum annealer. This may constrain the generality of applications, because not all machine learning algorithms can be transformed into combinatorial optimisation. The second drawback is the limitation of the problem size. The computational power offered by the currently available machine restricts the size to be quite small when comparing to what a conventional computer can solve nowadays. These imperfect properties nonetheless make the quantum annealing suitable to certain kind of machine learning that needs large amount of simple computations without requiring a high accuracy, such as boosting. To summarise, while machine learning has been identified as one of the areas where the quantum annealing technique may be useful, whether it will become a competitive player in the long run depends on the maturation of its hardware, which is the quantum annealer.

8 Conclusion

This work attempted to simulate a quantum annealer solving the 2-SAT problem at zero and finite temperature. After encoding the 2-SAT problem into the problem Hamiltonian, the simulation can be done by solving the time-dependent Schrödinger equation which describes the quantum annealing process.

For the zero temperature case, the first algorithm used is the full diagonalisation method. It is a straightforward approach and standard libraries, such as LAPACK, are available for diagonalising a matrix. The limitation is that the size of the problem cannot be large, otherwise the run time becomes too long. In spite of this, the full diagonalisation method can well serve as a validation for other algorithms solving the time-dependent Schrödinger equation. The second algorithm used is the Suzuki-Trotter product formula approach. With this approach, one can decompose a matrix exponential into a series of products of small matrix exponentials. If the analytical expressions of the small matrix exponentials are known, the simulation can be done without matrix diagonalisation. This approach is validated by the full diagonalisation method and then used to simulate an 8-spin system at zero temperature.

For the finite temperature case, the temperature effect is provided by coupling a heat bath to the system. The heat bath can be described by the canonical ensemble. The quantum annealing process of the entire system can then be simulated by running simulations over every energy state of the heat bath. The run time of this approach grows linearly with the number of energy states of the heat bath. Therefore, if the size of the heat bath is large, this approach cannot be considered practical. To reduce the run time of the simulation, the random sampling method is presented. The main assumption is that the heat bath can be approximated with a random initial state, which means the simulation can be done with this random initial state instead of all energy states. Although multiple runs are usually necessary in order to improve the accuracy, the random sampling method still reduces the run time of the simulation greatly.

The simulation results of quantum annealing at zero temperature matched what the Landau-Zener theory describes. The success probability decreases, when the minimum gap value gets smaller. This also indicates that the difficulty of a quantum annealing process can be estimated by its minimum gap value. The result at zero temperature also showed that for short annealing times, the system cannot end in the ground state of the problem Hamiltonian, which is described by the adiabatic theorem.

The simulation results of quantum annealing at finite temperature showed that the trend of the success probability can be explained by thermal equilibration. When the total annealing time is short, the heat bath has not yet influenced the system and the system can evolve coherently. If the total annealing time becomes longer, the heat bath and the system start to really interact with each other. The success probability reduces for longer total annealing times in this regime. If the total annealing time gets even longer, the entire system reaches a quasi-static state. As a result, the success probability increases with

longer total annealing times. The effect of a finite temperature and coupling strength lowers the overall success probability. Besides, the effect of both causes data to be scattered instead of being a smooth line described by the Landau-Zener formula.

In summary, quantum annealing provides a different approach to solve 2-SAT problems. Furthermore, this technique can be applied in other areas such as machine learning, if one can transform the algorithm into a proper form for a quantum annealer. While a practical use of the quantum annealer relies on the future maturation of the hardware, this work demonstrated some general properties of a quantum annealer when solving an optimisation problem and all simulations done in this work can be implemented in a quantum annealer for comparison.

References

[1] Richard P. Feynman. Simulating physics with computers. *International Journal of Theoretical Physics*, 21(6-7):467–488, 1982.

[2] Daniel R. Simon. On the power of quantum computation. *SIAM Journal on Computing*, 26(5):1474–1483, 1997.

[3] Peter W. Shor. Polynomial-time algorithms for prime factorization and discrete logarithms on a quantum computer. *SIAM Journal of Computing*, 26(5):1484–1509, 1997.

[4] Lov K. Grover. A fast quantum mechanical algorithm for database search. *Proceedings of the twenty-eighth annual ACM symposium on Theory of computing - STOC '96*, pages 212–219, 1996.

[5] Nicolas J. Cerf, Lov K. Grover, and Colin P. Williams. Nested quantum search and NP-hard problems. *Applicable Algebra in Engineering, Communications and Computing*, 10(4):311–338, 2000.

[6] Charles H. Bennett, Ethan Bernstein, Gilles Brassard, and Umesh Vazirani. Strengths and weaknesses of quantum computing. *SIAM Journal on Computing*, 26(5):1510–1523, 1997.

[7] T. D. Ladd, F. Jelezko, R. Laflamme, Y. Nakamura, C. Monroe, and J. L. O'Brien. Quantum computers. *Nature*, 464(7285):45–53, 2010.

[8] Dorit Aharonov, Wim van Dam, Julia Kempe, Zeph Landau, Seth Lloyd, and Oded Regev. Adiabatic quantum computation is equivalent to standard quantum computation. *SIAM Review*, 50(4):755–787, 2008.

[9] Edward Farhi, Jeffrey Goldstone, Sam Gutmann, and Michael Sipser. Quantum Computation by Adiabatic Evolution. *arXiv:quant-ph/0001106*, 2000.

[10] John A Smolin and Graeme Smith. Classical signature of quantum annealing. *Frontiers in Physics*, 2:52, 2014.

[11] J Brooke, D Bitko, T F., Rosenbaum, and G Aeppli. Quantum Annealing of a Disordered Magnet. *Science*, 284(5415):779–781, 1999.

[12] Guenter Gottstein. *Physical Foundations of Materials Science*, volume 2. Springer-Verlag Berlin Heidelberg GmbH, 2012.

[13] Arnab Das and Bikas K. Chakrabarti. Colloquium: Quantum annealing and analog quantum computation. *Reviews of Modern Physics*, 80(3):1061–1081, 2008.

[14] Demian A. Battaglia, Giuseppe E. Santoro, and Erio Tosatti. Optimization by quantum annealing: Lessons from hard satisfiability problems. *Physical Review E*, 71(6):1–10, 2005.

[15] Edward Farhi, Jeffrey Goldstone, Sam Gutmann, Joshua Lapan, Andrew Lundgren, and Daniel Preda. A Quantum Adiabatic Evolution Algorithm Applied to Random Instances of an NP-Complete Problem. *Science*, 292(5516):472–475, 2001.

[16] Sergio Boixo, Troels F Ronnow, Sergei V Isakov, Zhihui Wang, David Wecker, Daniel A Lidar, John M Martinis, and Matthias Troyer. Evidence for quantum annealing with more than one hundred qubits. *Nat Phys*, 10(3):218–224, 2014.

[17] M. S. Sarandy, L. A. Wu, and D. A. Lidar. Consistency of the adiabatic theorem. *Quantum Information Processing*, 3(6):331–349, 2004.

[18] Giuseppe E Santoro and Erio Tosatti. Optimization using quantum mechanics: quantum annealing through adiabatic evolution. *Journal of Physics A: Mathematical and General*, 39(36):R393–R431, 2006.

[19] Christos H. Papadimitriou and Kenneth Steiglitz. Combinatorial Optimization: Algorithms and Complexity. *The American Mathematical Monthly*, 91(3):209, 1984.

[20] H. De Raedt and K. Michielsen. Computational Methods for Simulating Quantum Computers. In M. Rieth and W. Schommers, editors, *Handbook of Theoretical and Computational Nanotechnology*, volume 3, chapter 1, page 248. American Scientific Publisher, Los Angeles, 2006.

[21] Anthony Hams and Hans De Raedt. Fast algorithm for finding the eigenvalue distribution of very large matrices. *Physical Review E*, 62(3):4365–4377, 2000.

[22] Mohammad H. Amin. Searching for quantum speedup in quasistatic quantum annealers. *Physical Review A*, 92(5):1–5, 2015.

[23] Edward Boyda, Saikat Basu, Sangram Ganguly, Andrew Michaelis, Supratik Mukhopadhyay, and Ramakrishna R Nemani. Deploying a quantum annealing processor to detect tree cover in aerial imagery of California. *Plos One*, 12(2):e0172505, 2017.

[24] Daniel O'Malley, Velimir V. Vesselinov, Boian S. Alexandrov, and Ludmil B. Alexandrov. Nonnegative/binary matrix factorization with a D-Wave quantum annealer. *arXiv:1704.01605*, 2017.

Declaration

Ich versichere, dass ich die Arbeit selbstständig verfasst und keine anderen als die angegebenen Quellen und Hilfsmittel benutzt sowie Zitate kenntlich gemacht habe.

Aachen, den